Chemical Geology 594 (2022) 120776

Contents lists available at ScienceDirect

Chemical Geology

journal homepage: www.elsevier.com/locate/chemgeo

Invited review article

The komatiite testimony to ancient mantle heterogeneity

Igor S. Puchtel [a,*], Janne Blichert-Toft [b], Mary F. Horan [c], Mathieu Touboul [b], Richard J. Walker [a]

[a] *Department of Geology, University of Maryland, 8000 Regents Drive, College Park, MD 20742, USA*
[b] *Laboratoire de Géologie de Lyon, Ecole Normale Supérieure de Lyon, CNRS UMR 5276, Université de Lyon, 46 Allée d'Italie, 69007 Lyon, France*
[c] *Earth and Planets Laboratory, Carnegie Institution for Science, 5241 Broad Branch Road NW, Washington, DC 20015, USA*

ARTICLE INFO

Editor: Catherine Chauvel

Keywords:
Komatiites and basalts
primordial magma ocean
early mantle heterogeneity
^{182}W, ^{142,143}Nd, ^{176}Hf, ^{186,187}Os isotope systems
siderophile elements
grainy late accretion
core-mantle interaction
mixing rates of the mantle
Nd-Hf-Os isotope paradox

ABSTRACT

Komatiites are crystallized samples of high-temperature, high-MgO lavas that were common during the Archean, but became increasingly rarer in the Proterozoic and Phanerozoic. Although the origin of komatiites remains a subject of debate, all komatiites included in this review, ranging in age from 3.6 to 2.0 Ga, are interpreted to have most likely been derived from anhydrous melting in mantle plumes. These plumes are estimated to have been initiated at different depths in the mantle, thus, providing important information about the chemical evolution of the early Earth.

The ^{142,143}Nd, ^{176}Hf, ^{182}W, ^{187}Os, and ^{186}Os systematics and trace- and highly siderophile element (HSE) abundances of these komatiites provide strong evidence for the presence of isotopic and chemical heterogeneities in the mantle during the first half of Earth history. These heterogeneities likely reflect the combined effects of (1) the co-existence of diverse post-magma ocean silicate domains that were characterized by variably-fractionated lithophile and siderophile element abundances; (2) the presence of distinct reservoirs that included mantles and cores of late accreted, differentiated planetesimals; and (3) isotopic exchange across the core-mantle boundary. These data highlight the complexity of komatiite mantle sources, none of which were similar in composition to estimates for the modern bulk silicate Earth (BSE). Moreover, no single petrogenetic model can account for the remarkably diverse chemical and isotopic compositions of komatiites.

The disappearance of resolvable positive and negative ^{142}Nd anomalies, as well as decoupled ^{143}Nd-^{176}Hf isotopic signatures, in the mafic-ultramafic rock record by ~2.5 Ga indicate that, by the end of the Archean, the earliest silicate reservoirs, formed through primordial magma ocean crystallization, had been largely destroyed as a result of vigorous convective mantle mixing. This implies that, during the Hadean and Archean, it took the mantle ~1.5 Ga to mix away the early formed ^{142}Nd heterogeneities *via* wholesale mantle convection. Similar to ^{142}Nd systematics, there appears to have been a shift from mostly positive ^{182}W anomalies in pre-2.5 Ga komatiite mantle sources to no ^{182}W offsets in post-2.5 Ga komatiite mantle sources. Coupled with the disapperance of projected HSE depletions in komatiite mantle sources at ~2.5 Ga, relative to the modern BSE, this shift may indicate that, by the end of the Archean, late accreted planetesimals had become largely homogenized within the mantle, and core-mantle interaction took over as the main driving force of creating ^{182}W isotope anomalies, possibly coincident with the timing of the onset of modern-style plate tectonics on Earth.

1. Introduction

Accurately determining how the distribution of chemical elements within the Earth has changed over time has been, and remains, one of the most fundamental challenges in Earth science; it has far-reaching implications not only for the long-standing debate about how terrestrial planets formed and evolved, but also for understanding ongoing processes on Earth. The information pertaining to the origin and early evolution of Earth comes largely from the geological rock record between ~4.0 and 2.0 Ga, which harbors isotopic and elemental signatures generated in the terrestrial reservoirs *via* early chemical fractionation processes and the radioactive decay of short- and long-lived refractory nuclides, including ^{146,147}Sm, ^{176}Lu, ^{182}Hf, ^{187}Re, and ^{190}Pt.

The mantle is the largest of all the terrestrial reservoirs. Its chemically and isotopically heterogeneous nature has long been established by numerous pioneering studies of the Earth's rock record (*e.g.,* Hart and Brooks, 1977; Hofmann and Hart, 1978; Zindler et al., 1982; Hart and Zindler, 1986; Zindler and Hart, 1986; Jacobsen, 1988; Galer and

---

* Corresponding author.
E-mail address: ipuchtel@umd.edu (I.S. Puchtel).

https://doi.org/10.1016/j.chemgeo.2022.120776
Received 23 August 2021; Received in revised form 6 February 2022; Accepted 15 February 2022

Goldstein, 1991). Some of the heterogeneities have been argued to be primordial in nature, reflecting initial planetary accretion/differentiation and magma ocean crystallization processes (Goldstein and Galer, 1992; Albarède et al., 2000; Drake, 2000; Boyet and Carlson, 2005; Frost et al., 2008; Caro, 2011; Touboul et al., 2012; Carlson et al., 2015; Jacobsen and Yu, 2015; Puchtel et al., 2016a; Rizo et al., 2016; Boyet et al., 2021). Others likely were formed as a result of a protracted terrestrial accretion history (*e.g.*, Willbold et al., 2011, 2015; Dale et al., 2017; Puchtel et al., 2018; Archer et al., 2019) or later processes associated with the dynamic regime of the planet, especially crustal recycling (*e.g.*, DePaolo, 1980; Armstrong, 1981; Hofmann and White, 1982; Patchett et al., 1984; Shirey and Hanson, 1986; Chase and Patchett, 1988; Galer et al., 1989; Bowring and Housh, 1995; Bennett et al., 1996; Salters and White, 1998; Blichert-Toft et al., 2015).

Despite these decades-long research efforts, still limited insights into the terrestrial mantle mixing history mean that the nature, origin, scale, and longevity of early mantle heterogeneities, in terms of different elements and isotopic systems, remain contentious. This review is intended to fill some of the existing gaps in our understanding of early Earth chemical evolution by synthesizing the existing short- and long-lived refractory radiogenic isotopic and elemental abundance data for a representative set of well-preserved and well-characterized komatiite and basalt systems that are especially advantageous for studying processes that occurred within the first 2.5 billion years of Earth history. In parallel, we address the question of the complex origins of komatiites and their usefulness as proxies for the chemical composition of the early Earth mantle.

Here, we consider komatiite-basalt systems from 13 different localities around the globe: the 3.55 Ga Schapenburg, 3.48 Ga Komati, and 3.26 Ga Weltevreden komatiites in the Kaapvaal Craton of South Africa; the 3.53 Ga Coonterunah, 3.34 Ga Kelly, and 3.18 Ga Ruth Well and Regal komatiites and basalts in the Pilbara Craton of Western Australia; the 2.82 Ga Kostomuksha, 2.41 Ga Vetreny, and 2.05 Ga Lapland komatiites in the Fennoscandian Shield of northern Europe; the 2.72 Ga Pyke Hill-Alexo and Boston Creek komatiites in the Superior Craton of Canada, and the 2.69 Ga Belingwe komatiites in the Rhodesian Craton of South Africa. These komatiite-basalt systems were chosen because of good preservation of their primary mineralogical and textural features and chemical and isotopic compositions, and because complete sets of published high-precision chemical and isotope data, obtained on the same sample sets, are available for these systems. A schematic world map showing the location of these komatiite-basalt systems is provided in the ***Electronic Supplement***.

2. Komatiites as probes of the early Earth mantle

Komatiites are ultramafic lavas containing more than 18% MgO in the parental liquid (Arndt and Nisbet, 1982). To be classified as a komatiite, the crystallized lava must either contain spinifex texture, or be genetically related to lavas containing spinifex texture. Spinifex texture is a crucial feature that distinguishes komatiites from other ultramafic lavas, such as picrites, boninites, and meimechites. It is characterized by the presence of large, skeletal crystals of olivine that form during rapid, *in situ* crystallization of high-MgO, superheated (*i.e.*, heated to above liquidus temperatures) silicate liquids. Due to the absence of nucleation sites, superheated liquids display a reluctance to nucleate, and olivine crystals that eventually form do so rapidly upon cooling below the liquidus and are typically large and skeletal, leading to the formation of spinifex texture (*e.g.*, Arndt, 1994; Arndt et al., 2008).

Ever since komatiites were first discovered and described in South Africa (Viljoen and Viljoen, 1969), these rocks have served as a source of valuable information bearing on the chemical and thermal evolution of the mantle (*e.g.*, Arndt et al., 2008). Owing to formation *via* the highest degrees of partial melting of all mantle-derived magmas, komatiites have compositions approaching that of mantle peridotite and, thus, represent the closest available approximation of the chemical characteristics of the mantle among volcanic rocks (*e.g.*, Arndt, 1977; Nesbitt et al., 1979; Herzberg, 1992). As high-degree, superheated, and low-viscosity melts, komatiites extracted large proportions of highly siderophile elements (HSE, including Re, Os, Ir, Ru, Pt, and Pd) from the mantle, experienced little differentiation prior to emplacement, and likely sampled mantle domains on the order of tens of millions of cubic kilometers, as evidenced by the sheer volumes of komatiitic magmas erupted in a number of Archean terrains. Some of these occurrences are argued to be similar in volume to recent and modern oceanic plateaus, such as the Ontong Java plateau (*e.g.*, Condie, 1975; Schubert and Sandwell, 1989; Storey et al., 1991; Kusky and Kidd, 1992; Desrochers et al., 1993; Kimura et al., 1993; Abbott, 1996; Kent et al., 1996; Puchtel et al., 1998; Arndt et al., 2001). During crystallization of komatiite lava flows, major and trace elements, including HSE, behaved in predictable manners relative to indices of magmatic differentiation, making it possible to obtain precise chronological information, estimate element mobility, and determine HSE abundances in the mantle sources of most komatiites. The ability of komatiites to provide a reliable record of the chemical and isotopic characteristics of mantle domains, that existed during the first half of Earth history, is the key underlying factor for focusing on komatiites in this review, which is intended to summarize what komatiites have taught us about the evolution of early Earth. On the other hand, although basalts are less informative as probes of the HSE characteristics of the mantle, because of their inherently higher Nd, Hf, and W abundances, they are shown here to be reliable recorders of mantle Nd, Hf, and W isotopic compositions and, therefore, have also been studied in several komatiite-basalt systems.

3. The analytical toolbox to study the chemical evolution of the mantle

The chemical evolution of the mantle has long been studied using radiogenic isotope systems and lithophile and siderophile element abundances in mantle-derived rocks. The lithophile element-based isotopic systems, particularly ^{142,143}Nd and ^{176}Hf, are, by way of their refractory nature and optimal half-lives, powerful tools for examining possible primordial magma ocean processes, as well as subsequent mantle melting and differentiation processes (*e.g.*, DePaolo and Wasserburg, 1976; Jacobsen and Wasserburg, 1979; Patchett and Tatsumoto, 1980; Patchett et al., 1981; White and Patchett, 1984; Zindler and Hart, 1986; Sivell and McCulloch, 1991). Silicate melts have lower Sm/Nd and Lu/Hf than co-existing silicate solids, and, after separation, evolve to distinctive ^{143}Nd and ^{176}Hf compositions. If Sm/Nd fractionated prior to ~4.0 Ga, while ^{146}Sm was still extant, variations in ^{142}Nd can also be generated. Hence, application of the combined ^{142,143}Nd systems provides the temporal resolution necessary for deciphering the timing and mechanisms of the earliest mantle differentiation events (Goldstein and Galer, 1992; Harper and Jacobsen, 1992; Boyet et al., 2003; Caro et al., 2003, 2006, 2017; Boyet and Carlson, 2005, 2006; Bennett et al., 2007; O'Neil et al., 2008, 2012, 2016; Rizo et al., 2012, 2013, 2016; Roth et al., 2013, 2014). Further, combining the ^{142,143}Nd with the ^{176}Hf systematics allows identification of specific processes that may have controlled mantle differentiation, including fractionation of the high-pressure bridgmanite (Mg-perovskite) and Ca-perovskite assemblage during crystallization of a primordial magma ocean (Caro et al., 2005; Hoffmann et al., 2011; Rizo et al., 2011; Puchtel et al., 2013, 2016a; Hoffmann and Wilson, 2017; Boyet et al., 2021).

The short-lived ^{182}Hf-^{182}W system can be used to detect fractionation of the lithophile trace element Hf from the siderophile trace element W occurring within the first ~60 Ma of Solar System history. This isotope system constitutes a high-resolution tool for identifying magma ocean crystallization, the effects of late accretion, and, by virtue of its dual lithophile and siderophile nature, potentially core-mantle interaction processes (Kleine et al., 2002, 2004, 2009; Yin et al., 2002; Jacobsen and Yu, 2015; Reimink et al., 2020; Willbold et al., 2011, 2015; Touboul et al., 2012; Puchtel et al., 2018, 2020, 2022; Rizo et al., 2019; Mundl-Petermeier et al., 2019, 2020). Further, application of the combined ^{142}Nd and ^{182}W tools can help discriminate between early magma ocean differentiation processes and the effects of late accretion (Harper and Jacobsen, 1996; Rizo et al., 2016, 2019; Puchtel et al., 2018; Peters et al., 2021).

Abundances of HSE, combined with ^{186}Os and ^{187}Os systematics, provide additional information about the chemical evolution of the mantle and the processes that operated early in Earth history (*e.g.*, Righter et al., 2000; Walker, 2009, 2016; Day, 2013; Puchtel et al., 2014; Day et al., 2016). The behavior of Re, Pt, and Os is governed by their strong partitioning into metal or sulfide liquids relative to silicate melt (Crocket et al., 1997; Righter and Drake, 1997). During mantle melting, Os is moderately to highly compatible with the melting residue, whereas Pt and Re are incompatible to various degrees (*e.g.*, Barnes et al., 1985; Rehkämper et al., 1999; Mallmann and O'Neill, 2007). Thus, the two Os isotopic systems, together with HSE abundances, provide insight into some primordial processes, to which the lithophile element-based isotopic systems are not sensitive, including late-stage planetary accretion and metal-silicate differentiation. Estimates of HSE abundances in komatiite mantle sources can also be used to track the mixing rates of the mantle and the timing of homogenization of late accreted materials within the mantle (*e.g.,* Maier et al., 2009; Puchtel et al., 2018, 2020, 2022). In combination with Os isotope systematics and HSE abundances, the ^{182}Hf-^{182}W isotopic system can be used to discriminate between the effects of early planetary differentiation, late accretion, and core-mantle interaction (*e.g.*, Touboul et al., 2012; Puchtel et al., 2016a, 2018, 2020, 2022; Archer et al., 2019; Rizo et al., 2019; Tusch et al., 2021).

The water content of a komatiitic lava is also an important parameter for assessing where in the mantle the parental melt originated. Water is highly incompatible during mantle melting (*e.g.*, Moore, 1970; Michael, 1995; Saal et al., 2002; Hauri et al., 2006; Cooper et al., 2012). The water content of a given komatiite mantle source can be derived from that of a komatiite lava provided that effects of secondary alteration can be corrected for. For example, correlations between the abundances of water and other lithophile trace elements, *e.g.*, Ce, in submarine basalt glasses have been used in a number of studies to establish H_2O contents of mantle-derived melts (*e.g.*, Michael, 1995; Saal et al., 2002; Hauri et al., 2006; Cooper et al., 2012). Mid-ocean ridge basalt (MORB) and ocean island basalt (OIB) magmas have $H_2O/Ce \leq 370$ (Hauri et al., 2006), similar to the mantle value of 200±50 (Hirschmann, 2018); the rather large range is due to the fact that during anhydrous mantle melting, spinel lherzolite has a bulk solid/melt $D_{H2O} \approx D_{Ce}$, whereas garnet lherzolite has a bulk solid/melt $D_{H2O} = 0.5 \times D_{Ce}$. By contrast, arc magmas have H_2O/Ce of 2,000 to 3,000, due to variable contributions of H_2O from the subducting slab (Cooper et al., 2012).

The oxidation state of a komatiite magma and its source reflects important information about the location and processes involved in its generation. For example, knowledge of fO_2 can potentially be used to distinguish between a hydrous (*i.e.*, subduction) versus anhydrous (*i.e.*, mantle plume) origin of komatiites. Canil (1997, 1999, 2002) and Canil and Fedortchouk (2001) used V partitioning between liquidus olivine and komatiitic melt as a redox indicator. These authors showed that the major factor controlling the partitioning of V between olivine and komatiitic melt ($D_V^{ol/liq}$) was oxygen fugacity, fO_2. More oxidized, water-rich island arc magmas (higher fO_2) are invariably characterized by $D_V^{ol/liq} < 0.01$, whereas less oxidized, anhydrous mantle plume-derived magmas (*e.g.*, OIB and MORB) exhibit $D_V^{ol/liq} = 0.025 - 0.10$.

Additional diagnostic features pointing to the origins of komatiites include estimates of potential temperatures of inferred mantle sources and depths of melting initiation. To compare mantle temperatures at various localities, McKenzie and Bickle (1988) proposed the concept of a mantle potential temperature ($\mathbf{T}_p$) as a point of reference. Mantle potential temperature is the temperature that the solid adiabatically-convecting asthenospheric mantle would have had at the surface if it ascended without undergoing melting. Mantle potential temperature determines the depth of melting initiation (*e.g.*, Richter, 1988; Herzberg, 1992, 1995; Herzberg et al., 2007), which, in turn, governs the style of mantle melting and melt segregation (fractional versus batch). The depth of melting initiation and subsequent melt segregation determines the chemical composition of the resultant komatiite melts, including MgO contents. Pressures >8 GPa (240 km depth) stabilize majorite garnet relative to olivine and pyroxene in the source (*e.g.*, Ohtani, 1984; Herzberg and Ohtani, 1988). If the temperature of a mantle plume is sufficiently high to initiate melting in the majorite garnet stability field, the melting results in the formation of Al-depleted komatiitic melts with subchondritic Al_2O_3/TiO_2 and Gd/Yb, provided the melt separated from the melting residue while still in the majorite garnet stability field. By contrast, melting and melt segregation at lower pressures, within the spinel lherzolite stability field, produces Al-undepleted komatiitic magmas with chondritic Al_2O_3/TiO_2 and Gd/Yb (*e.g.*, Green, 1975; Ohtani, 1984; Kato et al., 1988; Herzberg, 1995).

4. Which parts of the mantle do komatiites sample?

In order to assess the extents of early mantle isotopic and chemical heterogeneities sampled by komatiites, it is important to determine where in the mantle komatiites originated. The location of komatiite magma generation was almost certainly not the same for all komatiites, given the extent of chemical and isotopic heterogeneity inferred for their mantle sources. This, in turn, requires assessment of diverse komatiite formation models.

Komatiites were most common during the Archean and may, during that eon, have been the volumetrically second most significant constituent among volcanic rocks, comprising as much as 25% of the entire volume of volcanic sequences, the rest being composed mostly of basalts (*e.g.*, Condie, 1975, 1981, 1994; De Wit and Ashwal, 1997). Some of these basalts were also derived from komatiites *via* fractional crystallization processes, while others were lower-degree partial melts generated from the same sources, as the spatially associated komatiites (Arndt et al., 1977; Campbell et al., 1989; Condie, 2005). The abrupt decline in the abundance of komatiites at the Archean-Proterozoic boundary, as well as the decrease in the MgO contents of emplaced komatiite lavas, have been interpreted as evidence for a significant, up to 300°C, secular cooling of the mantle over the course of Earth history (*e.g.,* Bickle, 1982; Nisbet et al., 1993; Herzberg et al., 2007; Herzberg and Gazel, 2009). Some authors have linked this to a transition from drip- to subduction tectonics (Campbell and Griffiths, 2014), arguing that an increasing abundance of subducted slabs allowed for formation of the core-enveloping D″ insulating layer, which they in turn associate with a step-like drop in maximum komatiite magma MgO contents and mantle potential temperatures between 2.7 and 2.0 Ga.

The origin of komatiites has been a subject of intensive studies for the past half-century (*e.g.*, Green, 1975, 1981; Allègre, 1982; Arndt et al., 1998, 2008; Parman et al., 2001, 2004; Berry et al., 2008; Sobolev et al., 2016, 2019; Sossi et al., 2016; Asafov et al., 2018). A common interpretation is that the parental magmas to komatiites were produced in unusually hot upwellings of mantle material, termed mantle plumes (*e.g.*, Cawthorn, 1975; Campbell et al., 1989; Griffiths and Campbell, 1990; Richards et al., 1991; Loper, 1991; Herzberg, 1995; Richard et al., 1996). The plumes most likely initiated at one of the two major thermal boundary layers in the mantle, *i.e.*, either the core-mantle boundary (CMB) at 2900 km, or the 660 km discontinuity, with the ensuing rise driven by a buoyancy contrast between the less dense, hot plume material and the cooler and denser surrounding mantle (Campbell and Griffiths, 1990, 1992, 1993; Farnetani and Richards, 1995; Farnetani, 1997). The initially solid mantle plume material was partially melted upon reaching shallower depths as a result of decompression. Based on experimental data, Campbell et al. (1989) argued that komatiites were produced in the hotter plume core containing mostly materials derived from the region near the thermal boundary layer, whereas spatially associated basalts were generated in the cooler plume head which, upon arrival at the surface, would have contained a substantial amount of entrained upper mantle material. However, later studies (*e.g.*, Farnetani and Richards, 1995) argued that such entrainment was unlikely to contribute significantly to the erupted melts.

Two major types of modern mantle plumes have been proposed, based on the depth of their initiation determined using recent high-resolution seismic tomography imaging data (*e.g.*, Courtillot et al., 2003; Montelli et al., 2004; He et al., 2015; Bao et al., 2022). The first type is "primary", or Morganian, plumes, that are commonly thought to originate in the deepest parts of the lower mantle, perhaps from seismically anomalous regions. Early geophysical studies (*e.g.*, Dziewonski et al., 1977) identified seismically anomalous zones along the core-mantle boundary, the so-called Large Low Shear-Wave Velocity Provinces (LLSVP) and Ultra-Low Velocity Zones (ULVZ). The origin of these regions in the mantle is debated. It has been proposed that LLSVPs may be stratified into primordial bottom domains near the core-mantle boundary, often referred to as the D" layer, and mafic shallow domains that extend from ~1100 to 2300 km depths (*e.g.*, Ballmer et al., 2016; Koppers et al., 2021). These regions in the mantle may serve as nurseries for the majority of "primary" mantle plumes (French and Romanowicz, 2015; Torsvik et al., 2016; Koppers et al., 2021). Ocean island basalt systems that have been associated with this type of plumes include Azores, Canary, Coral Sea, Easter, Galapagos, Hawaii, Iceland, Samoa, and Tahiti (Courtillot et al., 2003).

The "secondary" type, or Andersonian plumes, have been proposed to originate at the 660 km discontinuity and, hence, would be an upper mantle feature. Ocean island basalt systems that have been associated with this type of plumes include Ascension, Caroline, McDonald, and Pitcairn islands (Courtillot et al., 2003).

Considering the difficulties in determining even present-day mantle plume characteristics (*e.g.*, Fletcher and Wyman, 2015, and references therein), it is not surprising that there are few reliable estimates of Archean plume parameters (Arndt et al., 2008). This is due to the fact that, unlike modern plumes, ancient plumes are extinct mantle features and, therefore, cannot be examined by geophysical methods. Consequently, indirect approaches must be taken, such as geological field observations. For example, the size of postulated plumes can potentially be constrained by the lateral extent of contemporaneous magmatic activity within a given region. Envisioned parental plume heads of up to 2500 km in diameter for large systems, such as the Yilgarn Craton in Western Australia (Campbell and Hill, 1988; Mole et al., 2014; Barnes and Van Kranendonk, 2014; Barnes et al., 2016), have been argued to be indicative of plumes that originated at the CMB. Smaller plume heads, estimated to range from 200 km to 300 km in diameter, and leading to less widespread volcanism, such as the komatiite-basalt systems of the Pilbara Craton in Western Australia and the Superior Craton in Canada (Arndt et al., 2001; Van Kranendonk, 2008; Hickman and Kranendonk, 2012; Dostal and Mueller, 2013; Wyman, 2013; Wyman, 2019; Wyman, 2020), are likely to be more typical of upper mantle plumes originated at the 660 km discountinuity.

Puchtel et al. (2009b, 2013, 2016a) calculated H_2O contents of <0.2 wt. % in the Pyke Hill, Belingwe, Schapenburg, Komati, and Weltevreden komatiites, and concluded that their parental magmas were formed under dry, high-temperature melting conditions. Similar estimates of water content have been obtained for the Belingwe komatiites on the basis of the oxidation state of iron in melt inclusions in olivine (*e.g.*, Berry et al., 2008). Thus, it is a common assumption that most komatiites originated from dry, deep-seated mantle sources (Arndt et al., 1998, 2008).

Consistent with the interpretation of an anhydrous, deep mantle origin for most komatiites, Nicklas et al. (2018, 2019) concluded, on the basis of a global survey of partitioning behavior of V between olivine and emplaced komatiitic and picritic melts, that the redox states of a variety of komatiite and OIB sources, ranging in age from 3.48 Ga to present day, were either similar to, or lower than, those of modern MORB.

Recent studies of komatiitic olivine melt inclusions (*e.g.*, Sobolev et al., 2016, 2019; Asafov et al., 2018), while maintaining an anhydrous, deep mantle plume origin for komatiites, have argued for relatively high water contents in some komatiite magmas, with water being added to rising, dry plume material from a thin hydrous layer located at the top of the mantle transition zone (MTZ), between the 410- and 660-km seismic discontinuities. The origin of these seismic interfaces is attributed to solid-solid phase transitions from olivine to wadsleyite and ringwoodite to perovskite+magnesiowüstite, respectively (*e.g.,* Bina and Helffrich, 1994). The hydrous layer is predicted by Bercovici and Karato (2003) in their MTZ water filter model to occur at the 410 km depth.

Alternatively, it has been argued that komatiites in general, and Komati lavas from the Kaapvaal Craton in South Africa in particular, were produced in a special type of Archean subduction environment *via* hydrous melting of the mantle at shallow depths and at temperatures similar to, or only slightly higher than, those of the ambient upper mantle (*e.g.*, Allègre, 1982; Grove et al., 1997; Parman et al., 1997, 2001, 2004). An important initial condition of this hypothesis is the requirement that the Komati komatiites represent intrusive bodies, since magmatic water escapes outgassing only under pressure (Grove et al., 1997). According to the hydrous komatiite model of Parman et al. (1997, 2001), the presence of water determined both the crystallization sequence and composition of the magmatic minerals of the Komati komatiites. Parman et al. (1997) carried out a detailed experimental study crystallizing material of komatiitic composition under both anhydrous and hydrous conditions, paying particular attention to the composition of the crystallizing pyroxene. Using the pyroxene compositions, these authors estimated that the original Komati komatiite magma contained between 4 and 6 wt. % H_2O. Such a large amount of water would require the temperature in the Komati source to be ~250°C lower than in anhydrous melting models. In their follow-up review paper, Grove and Parman (2004) argued that the Archean mantle was ≤100°C hotter than the modern mantle, hence, offering a view on the thermal evolution of the Earth that contrasts with those that are based on the traditional assumption of a substantially hotter Archean mantle (*e.g.*, Richter, 1985, 1988; Bickle, 1986; Nisbet et al., 1993; Herzberg et al., 2007, 2010).

The summary of estimates of the mantle potential temperatures (**T_p°C**) for the sources of the komatiite systems considered here, as well as the liquidus temperatures of the emplaced komatiite magmas (**T_{liq}°C**) and depths of melting initiation in the respective mantle plumes (**$D_{melt\ init}$**), are presented in Table 1. These estimates were generally derived from the studies for the particular komatiite systems referenced in Table 1 and updated here on the basis of the more recent estimates of the emplaced komatiite lava compositions from Nicklas et al. (2018, 2019), where available, coupled with the previous and more recent mantle melting parameterization models of McKenzie and Bickle (1988), Herzberg and O'Hara (2002), Herzberg and Asimow (2008), and Herzberg and Gazel (2009).

5. Chemical and isotopic data

A summary of the available chemical and isotopic data for the komatiite systems considered in this review are given in Tables 1 and 2.

5.1. *Emplaced lava compositions, mantle potential temperatures, and depths of melting*

Estimates of emplaced komatiite lava compositions (**MgO_{liq}**), their liquidus temperatures (**T_{liq}°C**), mantle potential temperatures (**T_p°C**), and depths of mantle melting initiation (**$D_{melt\ init}$**) are listed in Table 1. The details of the methodology used for calculating these parameters are provided in the ***Electronic Supplement***.

The calculated depths of melting initiation range between 605 and 203 km, while liquidus temperatures vary between 1606°C and 1498°C. There is an apparent tendency for a decrease in depth of melting

Table 1
Summary of ages, thermodynamic parameters, and chemical features of the komatiite systems considered in this review.

Komatiite-basalt system	Age, Ga	MgO$_{liq}$	T$_{liq}$°C	T$_p$°C	D$_{melt\ init,\ km}$	D$_{plume\ init}$	Al$_2$O$_3$/TiO$_2$	(La/Sm)$_N$	(Gd/Yb)$_N$	Nb/Nb*	W/Th
Kaapvaal Craton, South Africa											
Schapenburg	3.55	29.1±2.8	1582	1811	443	LM	10.0±0.8	0.93±0.04	1.57±0.10	1.2±0.1	9.7±5.5
Komati	3.48	29.9±0.5	1591	1822	494	LM	10.1±0.7	0.97±0.24	1.39±0.05	1.1±0.2	0.25±0.18
Weltevreden	3.26	31.4±0.9	1606	1841	605	LM	29.2±1.1	0.68±0.06	0.84±0.03	1.4±0.1	1.5±1.4
Pilbara Craton, Western Australia											
Coonterunah	3.53	23.0±0.3	1498	1705	203	MTZ	23.8±1.7	0.80±0.04	0.96±0.04	1.08±0.02	0.91±0.62
Kelly	3.34	27.4±1.0	1561	1786	351	MTZ	22.1±1.7	0.65±0.02	0.91±0.04	1.03±0.04	0.81±0.69
Ruth Well	3.18	29.3±0.7	1584	1814	455	MTZ	11.0±0.5	0.55±0.09† *0.77±0.09*	1.31±0.04† *1.32±0.04*	1.0±0.1† *0.51±0.05*	3.4±2.3
Regal	3.18	29.3±0.7	1584	1814	455	MTZ	11.9±0.8	0.61±0.11† *0.83±0.11*	1.28±0.12† *1.31±0.12*	1.0±0.1† *0.55±0.09*	3.5±2.8
Fennoscandian Shield, northern Europe											
Kostomuksha	2.82	27.6±1.0	1564	1789	361	LM	17.2±1.2	0.48±0.13	1.16±0.02	1.2±0.1	0.84±0.32
Vetreny	2.41	27.0±1.0	1556	1779	333	MTZ	19.7±0.5	0.41±0.10† *2.2±0.1*	1.2±0.1† *1.3±0.1*	1.0±0.1† *0.29±0.03*	0.05±0.02
Lapland	2.05	25.2±0.5	1532	1748	264	LM	13.9±0.4	0.14±0.02† *0.26±0.01*	1.48±0.02† *1.49±0.02*	1.0±0.1† *0.58±0.01*	0.16±0.06
Superior Craton, Canada											
Boston Creek	2.72					MTZ	5.1±0.8	1.9±0.3	2.0±0.2	1.2±0.2	0.9±1.4
Pyke Hill-Alexo	2.72	28.2±0.5	1571	1789	392	MTZ	20.4±0.6	0.53±0.16	0.98±0.03	1.0±0.1	0.15±0.06
Rhodesian Craton, Zimbabwe											
Belingwe	2.69	25.6±0.5	1537	1755	277	MTZ	19.8±0.6	0.68±0.02	1.02±0.04	0.97±0.05	0.20±0.06

†Values corrected for AFC. The italicized values are those measured in the emplaced lavas, before correction for AFC. All uncertainties are 2SD of the mean. MgO$_{liq}$ – the MgO content of the original emplaced komatiite magma for each komatiite system compiled from Nicklas et al. (2018, 2019) and Puchtel et al. (1998, 2016a, 2020, 2022). T$_{liq}$°C, T$_p$°C – liquidus temperatures of the emplaced komatiite magmas and mantle potential temperatures for the studied komatiite systems. D$_{melt\ init}$ – depths of melting initiation. D$_{plume\ init}$ – inferred depths of plume initiation for the studied komatiite systems. Nb/Nb* = $Nb_N/\sqrt{(Th_N \times La_N)}$, where N are the BSE normalizing values from Hofmann (1988). For sources of the data see Table 2. See text and the *Electronic Supplement* for details.

Table 2
Summary of isotopic features and HSE abundances of the komatiite systems considered in this review

Komatiite-basalt system	ε^{143}Nd(T)	ε^{176}Hf(T)	μ^{142}Nd	μ^{182}W	γ^{187}Os(T)	μ^{186}Os(T)	∑HSE	Data source
Kaapvaal Craton, South Africa								
Schapenburg	+2.4±0.5	+5.8±0.8	–5.0±2.8	–8.4±4.1	+3.7±0.3		29±9	[1 – 2]
Komati	+0.46±0.39	+1.9±1.0	–0.9±2.7	+2.7±4.5	+0.3±0.3	–12±8	60±8	[3 – 5]
Weltevreden	+0.54±0.40	+4.7±2.1	+2.5±3.8		–0.1±0.2	+22±7	65±6	[3 – 4]
Pilbara Craton, Western Australia								
Coonterunah	+2.4±0.5	+4.4±0.3		+11.4±4.6			29±6	[6]
Kelly	+0.5±0.6	+1.7±0.6		+8.2±3.3	+0.8±0.4		38±7	[6]
Ruth Well	+1.3±0.7† *+0.6±0.7*	+2.4±0.4† *+1.7±0.4*	–1.8±3.8	+7.7±5.0	–0.4±0.4† *–0.4±0.4*		55±4	[6]
Regal	+1.9±0.3† *+1.0±0.3*	+4.6±0.8† *+4.1±0.8*		+7.7±5.0	+0.9±0.3† *+0.9±0.3*		70±5	[6]
Fennoscandian Shield, northern Europe								
Kostomuksha	+3.0±0.4	+4.9±0.3	+0.4±0.9	+15.0±4.8	+2.5±0.6	+22±6	79±6	[7 – 11]
Vetreny	+3.7±0.4† *–0.9±0.4*	+6.3±0.9† *+0.4±0.9*	+0.5±2.1	–0.5±5.2† *+7.5±5.2*	+1.3±0.2† *+1.7±0.2*	+3.2±1.7	66±10	[12]
Lapland	+4.9±0.3† *+3.7±0.3*	+10.2±0.7† *+8.7±0.7*		–10.0±5.0† *+1.5±3.3*	–0.2±0.3† *–0.2±0.3*	+29±2	120±5	[13]
Superior Craton, Canada								
Boston Creek	+2.5±0.2	+4.3±0.9	–3.8±2.8	+11.7±4.5	+0.1±0.3		35±10	[14]
Pyke Hill-Alexo	+3.0±0.5	+5.5±0.6	+6.8±2.5		+0.4±0.1	–0.1±4.2	85±5	[15 – 19]
Rhodesian Craton, Zimbabwe								
Belingwe	+2.9±0.2		+3.7±7.0		+0.1±0.2	+0.6±2.5	57±7	[20 – 21]

†Values corrected for AFC. The italicized values are those measured in the emplaced lavas, before correction for AFC. All uncertainties are 2SD of the mean. Data sources are as follows: [1] - Puchtel et al. (2009a); [2] - Puchtel et al. (2016a); [3] - Puchtel et al. (2013); [4] - Puchtel et al. (2014); [5] - Touboul et al. (2012); [6] - Puchtel et al. (2022); [7] - Puchtel et al. (1998); [8] - Boyet and Carlson (2006); [9] - Touboul et al. (2012); [10] - Puchtel et al. (2005); [11] - Puchtel and Humayun (2005); [12] - Puchtel et al. (2016b); [13] - Puchtel et al. (2020); [14] - Puchtel et al. (2018); [15] - Blichert-Toft and Arndt (1999); [16] - Puchtel et al. (2004a); [17] - Puchtel et al. (2004b); [18] - Puchtel et al. (2009b); [19] - Debaille et al. (2013); [20] - Puchtel et al. (2009b); [21] - Boyet and Carlson (2006).

initiation between 3.6 and 2.0 Ga. This is also reflected in the ~100°C decrease in mantle potential temperatures of komatiite sources from 1841 to 1748°C and a corresponding decrease in MgO contents of emplaced komatiite lavas from ~31 to 25 wt.% over the same period of time. Two exceptions are the Coonterunah and Kelly komatiite systems that are less MgO-rich than the other early Archean systems. Therefore, the data place the depths of onset of melting for all komatiite systems considered here within and above the present-day MTZ and provide the minimum estimates for the depths of mantle plume initiation (**D$_{plume\ init}$**). In the following sections, more clues, as to which parts of the mantle the studied komatiite systems sampled (*i.e.,* depths of mantle plume initiation), will be considered using the available geochemical and isotopic data (Table 2).

5.2. Chemical composition and isotopic systematics

5.2.1. Major and lihophile trace elements

The petrologically most important chemical element in komatiites, along with Mg, is Al; as a result, variations in Al_2O_3, and its rare earth element (REE) behavioral equivalent Yb, form an integral part of all komatiite classifications (*e.g.*, Nesbitt et al., 1979; Jahn et al., 1982). The komatiite systems reviewed here can be subdivided into two major petrological groups on the basis of their Al_2O_3 and Yb contents at a given MgO content, namely Al-depleted/enriched and Al-undepleted. The majority of the early Archean komatiite systems, including the Schapenburg, Komati, Weltevreden, Ruth Well, and Regal systems, belong to the Al-depleted/enriched type of lavas characterized by either sub- or supra-chondritic Al/Ti and Gd/Yb ratios (Table 1). Exceptions are the Coonterunah and Kelly systems that belong to the Al-undepleted type of lavas with $Al_2O_3/TiO_2 = 22.8$ and 23.1 and $Gd/Yb_N = 0.96$ and 0.91, respectively (where N denotes values normalized to BSE abundances of Hofmann, 1988). By contrast, the majority of the late Archean komatiite systems, including the Pyke Hill-Alexo, Belingwe, Vetreny, and Lapland systems, belong to the Al-undepleted type of lavas characterized by generally chondritic Al/Ti and Gd/Yb ratios. The Boston Creek (Puchtel et al., 2018) and Kostomuksha komatiites (Puchtel et al., 1998), with $Al_2O_3/TiO_2 = 5.1$ and 17.2 and $Gd/Yb_N = 2.0$ and 1.2, respectively, are notable exceptions. Although the Lapland komatiites have low $Al_2O_3/TiO_2 = 13.9$ and high $Gd/Yb_N = 1.5$, these features have been argued to be the result of enrichment in Ti and middle REE (MREE), rather than depletions in Al and heavy REE (Puchtel et al., 2020).

Owing to their high liquidus temperatures and low viscosities, komatiitic liquids are highly susceptible to contamination by upper crustal rocks during their passage through and/or emplacement onto the continental crust (Huppert et al., 1984; Huppert and Sparks, 1985). Archean upper crustal rocks are strongly enriched in Th, U, and light REE (LREE), and relatively depleted in Nb (Rudnick and Gao, 2014) as a result of subduction zone processes involving retention of Nb-rich rutile in the eclogitic residue (Foley et al., 2000; Rudnick et al., 2000). Because of that, upper crustal rocks are characterized by negative Nb anomalies relative to elements with similar incompatibility during mantle melting (Th and La), *i.e.*, their $Nb/Nb^* << 1.0$ (where $Nb/Nb^* = Nb_N/\sqrt{(Th_N \times La_N)}$). By contrast, primary komatiitic magmas are expected to have $Nb/Nb^* \geq 1.0$ (*e.g.*, Hofmann et al., 1986; Jochum et al., 1991). Due to large differences in highly incompatible lithophile trace element concentrations between the upper crust and komatiitic melts, crustal contamination usually leads to sharp increases in the abundances of Th, U, W, and LREE, but much less so of Nb, in the hybrid melts, which acquire negative Nb anomalies in the process. Hence, the Nb/Nb* ratio represents a diagnostic tool that has been utilized to evaluate and mathematically correct for the effects of crustal contamination (*e.g.*, Puchtel et al., 2016b, 2020, 2022).

The majority of the komatiite systems considered here are variably depleted in highly incompatible lithophile trace elements, with the La/Sm_N ratios ranging between 0.14 (the 2.05 Ga Lapland system) and 0.97 (the 3.48 Ga Komati system). The 2.72 Ga Boston Creek lavas are the sole exception ($La/Sm_N = 1.9$). Furthermore, all komatiite systems examined here have $Nb/Nb^* \geq 1.0$, reflecting either a lack of crustal contamination, or that the effects of crustal contamination have been mathematically corrected for, as indicated in Table 2. The details of the correction protocol are provided in the ***Electronic Supplement***.

5.2.2. *Isotopic systems of the lithophile elements*

Table 2 presents the initial ε^{143}Nd and ε^{176}Hf values (defined as the deviation in parts per 10,000 of initial ^{143}Nd/^{144}Nd and ^{176}Hf/^{177}Hf in a given sample from those in the chondritic reference at the time of lava emplacement) for each komatiite system, which represent compositions of the respective komatiite-basalt mantle sources. These values were derived from the respective Sm-Nd and Lu-Hf isochrons obtained for each komatiite-basalt system and, where appropriate, corrected for crustal contamination, as indicated in Table 2, using the lithophile trace element systematics discussed in the previous section. The resultant initial ε^{143}Nd and ε^{176}Hf values are all positive, ranging between +0.46 and +4.9 and +1.7 and +10.2, respectively, indicating that all the komatiite-basalt systems considered were derived from mantle sources with time-integrated supra-chondritic Sm/Nd and Lu/Hf.

By contrast, Blichert-Toft et al. (2015) reported ^{143}Nd and ^{176}Hf data for a suite of altered Komati drill core samples from several lava flows. That study produced a much greater scatter, and both positive and negative initial ε^{143}Nd and ε^{176}Hf values for whole-rock samples, than for the initial values obtained from the individual Sm-Nd and Lu-Hf isochrons for the remarkably well preserved Komati komatiite samples from the Puchtel et al. (2013) study reported in Table 2. Blichert-Toft et al. (2015) also reported data for variably leached clinopyroxene separates, which yielded initial ε^{143}Nd and ε^{176}Hf values of –2 and +5, respectively. This may indicate a more complex magmatic and/or alteration history of the samples studied by Blichert-Toft et al. (2015) than for the Komati samples studied by Puchtel et al. (2013).

The model-specific, time-integrated Sm/Nd and Lu/Hf ratios in the mantle sources of komatiite systems, derived from the respective Sm-Nd and Lu-Hf isochron sets, are plotted in Fig. 1. These ratios were calculated by assuming the minimum-degree fractionation from either the chondritic values or the values defined by the combined ^{142,143}Nd systematics (where available) to those required to bring the ε^{143}Nd and ε^{176}Hf to the measured initial ε^{143}Nd and ε^{176}Hf of the respective mantle sources by the time of komatiite-basalt system formation. All of these komatiite systems were derived from mantle sources having time-integrated ^{147}Sm/^{144}Nd and ^{176}Lu/^{177}Hf ratios between those of CHUR and DMM. An important feature of the data is that, while all komatiite-basalt systems younger than ~3.0 Ga follow the terrestrial Nd-Hf mantle evolution array, indicating long-term "coupled", or congruent, behavior of the Nd and Hf isotope systematics in the post-3.0 Ga komatiite mantle sources, the komatiite systems older than ~3.0 Ga (with the exception of the Pilbara Craton komatiite-basalt systems) plot above the terrestrial evolution curve, indicating long-term "decoupled", or incongruent, behavior of the Nd and Hf isotope systematics in their mantle sources. All these early Archean systems are from the Kaapvaal Craton in South Africa. The processes that might have been responsible for producing such Nd-Hf isotope decoupling are discussed in Section 6.1.

Relatively limited ^{142}Nd data are available for the komatiite systems reviewed in this study (Table 2). The komatiite systems, for which these data are available, mostly exhibit μ^{142}Nd values indistinguishable from the standard reference value, where μ^{142}Nd is defined as the deviation in parts per million of ^{142}Nd/^{144}Nd in a given komatiite sample from the laboratory reference materials (*AMES* or *JNdi*), which are considered to represent the composition of the modern BSE. The Schapenburg and Komati komatiite systems have small μ^{142}Nd deficits, averaging –5.0 ±2.8 (2SD; Puchtel et al., 2016a) and –4.0±4.1 (2SD; Boyet et al., 2021), respectively.

5.2.3. *Tungsten abundance and isotope systematics*

The ^{182}W data are reported as μ^{182}W, which is the deviation in parts per million of ^{182}W/^{184}W in a given sample from that of the in-house *Alfa Aesar* laboratory W reference material. The μ^{182}W value of 0 for the reference material is considered to represent the composition of the BSE. This is based on the observation that a limited number of data for modern MORB (Willbold et al., 2011; Rizo et al., 2016; Mundl et al., 2017), numerous data for OIB with low ^{3}He/^{4}He (Mundl-Petermeier et al., 2020), and data for Proterozoic and Phanerozoic glacial diamictites and granites (Mundl et al., 2018; Nakanishi et al., 2021) are all characterized by μ^{182}W values of ~0.

In contrast to ^{142}Nd, the majority of komatiite systems examined here exhibit either positive (all the Pilbara, the Kostomuksha, and the Boston Creek komatiite systems), or negative (the Schapenburg and Lapland komatiite systems) ^{182}W anomalies, with only the Komati and Vetreny komatiite systems lacking an ^{182}W anomaly.

The behavior of W during magmatic processes is governed mainly by the redox state of the magmatic system in question (Newsom et al., 1996; Arevalo and McDonough, 2008; König et al., 2011). Under

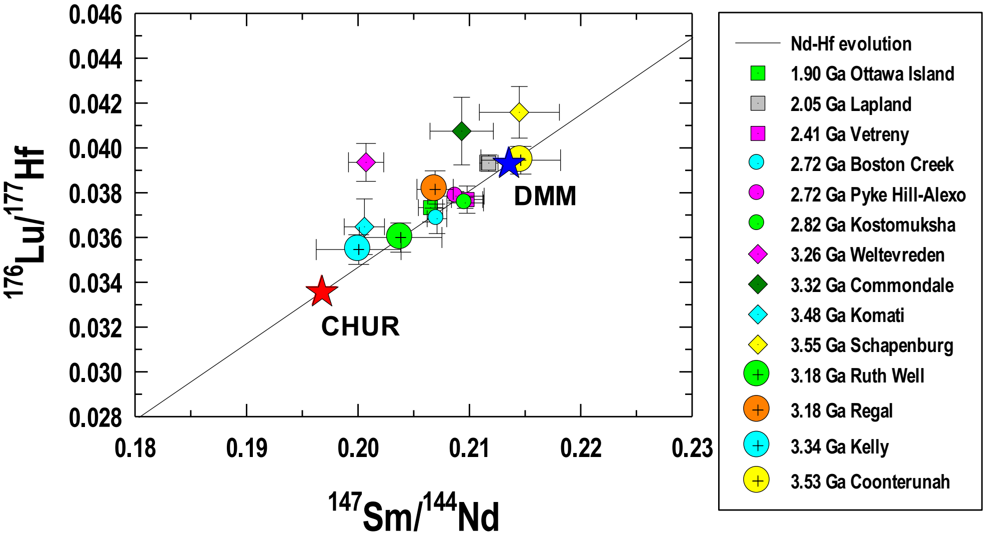

Fig. 1. Variations of model-specific (see the references below for the specific models used), time-integrated Sm/Nd and Lu/Hf ratios in the mantle sources of Archean and Proterozoic komatiite-basalt systems studied to date. The individual models assume a minimum-degree fractionation of Sm/Nd and Lu/Hf in the particular mantle domains from either the chondritic values or values defined by the combined ^{142,143}Nd/^{144}Nd systematics (where available) to those required to bring the ε^{143}Nd and ε^{176}Hf in the mantle sources to the initial ε^{143}Nd and ε^{176}Hf by the times of the respective komatiite formation. The solid line connects Sm/Nd and Lu/Hf ratios inferred for the chondritic uniform reservoir (CHUR) and modern depleted mantle (DMM). Data are from: Ottawa – Blichert-Toft and Arndt (1999); 2.05 Ga Lapland – Puchtel et al. (2020); 2.41 Ga Vetreny – Puchtel et al. (2016b); 2.72 Ga Pyke Hill and Alexo – Dupré et al. (1984), Walker et al. (1988), Blichert-Toft and Arndt (1999); 2.72 Ga Boston Creek – Puchtel et al. (2018); 2.82 Ga Kostomuksha – Puchtel et al. (1998), Blichert-Toft and Puchtel (2010); 3.48 Ga Komati and 3.26 Ga Weltevreden – Puchtel et al. (2013); 3.32 Ga Commondale – Wilson and Carlson (1989), Hoffmann and Wilson (2017); 3.55 Ga Schapenburg – Puchtel et al. (2009a, 2016a); 3.53 Ga Coonterunah, 3.34 Ga Kelly, and 3.18 Ga Ruth Well and Regal – Puchtel et al. (2022). The CHUR and DMM parameters are from Jacobsen and Wasserburg (1980), Hamilton et al. (1983), Goldstein et al. (1984), Vervoort and Blichert-Toft (1999), and Bouvier et al. (2008). All uncertainties are 2SD of the mean.

reducing conditions, such as those that likely existed during metallic core formation, W behaves as a moderately siderophile element (MSE), concentrating largely in the metal relative to the silicate melt. During mantle melting under relatively oxidizing conditions in the absence of a metal phase, such as typical of the modern upper mantle, W behaves as a highly incompatible element, concentrating in the silicate melt relative to the melting residue, with a degree of incompatibility similar to that of Th and U.

The Archean mantle was recently shown to be only slightly (by ~1.3 ΔFMQ log units) less oxidized than, whereas the Proterozoic mantle was found to be similarly oxidized to, the modern mantle (Nicklas et al., 2018, 2019). Therefore, it is expected that during mantle melting that produced the komatiite-basalt systems considered in this review, W behaved similarly to Th and U and, hence, that in undisturbed komatiite-basalt systems, W/Th ≈ W/Th$_{BSE}$, where W/Th$_{BSE}$ = 0.19 (McDonough and Sun, 1995). Indeed, in modern OIB and MORB, for which W is characterized by a primary, magmatic distribution, the W/Th ratios are similar to the BSE value of 0.19 (*e.g.*, König et al., 2008, 2011; Jenner et al., 2012). Modern island arc lavas, on the other hand, show uniformly elevated W/Th ratios relative to the BSE value, which is attributed to various constributions of fluid-borne W to the arc mantle from the subducted slab (König et al., 2008, 2011). Although some komatiite systems (*e.g.*, the Komati, Vetreny, and Lapland systems) have average W/Th ratios within the uncertainty limits of the BSE value, and in that respect are similar to modern OIB and MORB, others are variably either enriched (most common) or depleted in W over Th (Table 1). In addition, the lack of correlation between W concentrations and indices of magmatic differentiation, such as MgO content, indicates either W mobility after lava emplacement in most komatiite-basalt systems (*e.g.*, Touboul et al., 2012; Puchtel et al., 2016a, 2018, 2020, 2022; Tusch et al., 2021) or involvement of a yet-unaccounted-for magmatic process.

The issue of the origin of W in Archean and Proterozoic komatiite-basalt systems is, therefore, controversial. Recent studies have shown that W abundance and isotopic systematics can be affected by crustal contamination, hydrothermal alteration, and metamorphism (*e.g.*, Touboul et al., 2014; Liu et al., 2016; Puchtel et al., 2016a, 2016b, 2018, 2020, 2022; Tusch et al., 2019, 2021), resulting mostly in W enrichments relative to immobile trace elements with similar degree of incompatibility, *e.g.*, Th. Two mechanisms, based on the origin of W, have been proposed to account for the elevated W/Th ratios in komatiites and basalts. The first mechanism advocates derivation of W from an endogenous source, whereby W originated within the komatiite-basalt system. The second mechanism assumes an exogeneous origin, whereby W is introduced into the komatiite-basalt systems from genetically unrelated sources. We address these two mechanisms in more detail below.

Endogenous origin of W in komatiite-basalt systems have been advocated for the Kostomuksha (Touboul et al., 2012), Schapenburg (Puchtel et al., 2016a), Boston Creek (Puchtel et al., 2018), and the Coonterunah and Kelly systems (Puchtel et al., 2022). In the case of the two Pilbara komatiite-basalt systems, the komatiites are characterized by high W/Th ratios, whereas the basalts, which are spatially associated and genetically related to the komatiites, are depleted to only slightly enriched in W relative to Th. In these komatiite-basalt systems, and also in many other Archean komatiite-basalt systems around the globe, komatiites constitute 5-10% of the sequence by volume, the rest consisting of basalts (Condie, 1981; de Wit and Ashwal, 1997; Smithies et al., 2007). Originally, basalts contain significantly higher abundances of all highly incompatible trace elements, including W, compared to komatiites. During secondary alteration, komatiites are turned into serpentinites, whereas basalts are transformed into amphibolites. Serpentine is a major host for W and can accommodate several orders of magnitude more W than the precursor mineral olivine, whereas W shows a lower affinity for amphibole (Liu et al., 2016). Therefore, if W is mobilized and redistributed within a komatiite-basalt volcanic sequence, it is expected to be preferentially captured by komatiites during serpentinization of the primary mineral assemblage. The effect of this relative W enrichment is amplified by the low trace element concentrations in komatiites, resulting in high W/Th ratios (Puchtel et al., 2022).

In the case of the Boston Creek system, samples collected across a differentiated lava flow have remarkably uniform ^{182}W compositions, but show a wide range of W/Th ratios, from enriched in the lower olivine cumulate part to BSE-like in the low-Mg basaltic layer, with strong inverse correlation between MgO content (*i.e.*, amount of modal serpentine) and W/Th (Puchtel et al., 2018). The above features were argued by these authors to reflect an endogenous nature of W in the Boston Creek system, with isotopically uniform W having been redistributed within the lava flow and, hence, reflecting the primary magmatic signature.

The above scenarios have been argued to be applicable to several other komatiite-basalt systems, including the Kostomuksha (Touboul et al., 2012), and the Schapenburg (Puchtel et al., 2016a) systems.

Exogenous W in the komatiite-basalt systems considered in this review has been shown to be derived from upper crustal rocks either during passage of mafic-ultramafic magmas through the continental crust *en route* to the surface (the Vetreny and Lapland systems: Puchtel et al., 2016b, 2020), or as a result of interaction with upper crustal rocks during both the magmatic stage *via* crustal contamination, and the post-magmatic stage *via* fluid-rock interaction (the Ruth Well and Regal systems: Puchtel et al., 2022).

Due to the generally high W abundances in upper crustal rocks (*e.g.*, Rudnick and Gao, 2014), crustal contamination has the potential to modify both W concentrations and ^{182}W compositions of komatiite-basalt magmas during ascent, as has been argued to be the case for the Vetreny, Lapland, Ruth Well, and Regal systems on the basis of studies of lithophile trace element systematics (Puchtel et al., 2016b, 2020, 2022). In order to mathematically correct for the effects of magmatic crustal contamination, these authors performed un-mixing calculations using the degrees of crustal contamination estimated on the basis of trace element systematics and assumptions about the W isotopic composition and abundances in the most likely potential crustal contaminant.

Being a highly fluid-mobile element (*e.g.*, König et al., 2008), W can be transferred from spatially associated granitic rocks to komatiite-basalt sequences *via* W-rich fluids. Such a mechanism has been proposed to affect the W isotopic composition of the Ruth Well and Regal komatiite systems on the basis of the high W/Th ratios in both komatiites and basalts and the similarity in ^{182}W compositions between the most W-enriched komatiites and the spatially associated 3.5 Ga tonalites of the Pilbara Craton (Puchtel et al., 2022). These authors were able to evaluate the W isotopic composition of the primary lavas by assuming that their ^{182}W composition was similar to that of the least affected basalts from Tusch et al. (2021) and Puchtel et al. (2022), with W/Th ratios closest to that in the BSE estimate.

After corrections have been applied, where needed, the μ^{182}W values reported in Table 2 are considered to reflect those in the sources of the respective komatiite-basalt systems.

5.3. Os isotope systematics and HSE abundances

The ^{186,187}Os data are listed in Table 2 and plotted in Fig. 2. The majority of the komatiite systems have γ^{187}Os values (defined as per cent deviation of the ^{187}Os/^{188}Os ratio in a given komatiite sample from a chondritic reference value at the time of komatiite lava emplacement) plotting within the chondritic range, indicating evolution of their mantle sources with time-integrated near-chondritic Re/Os ratios. The only exceptions are the Schapenburg and Kostomuksha komatiite systems that have more radiogenic γ^{187}Os values of +3.7 and +2.5, respectively, implying that their mantle sources evolved with long-term slightly supra-chondritic Re/Os.

The limited ^{186}Os data available indicate that, out of the seven systems studied, only three (the Pyke Hill, Belingwe, and Vetreny systems) have initial μ^{186}Os values (defined as the deviation in parts per million of the ^{186}Os/^{188}Os ratio in a given komatiite sample from a chondritic reference value at the time of the komatiite lava emplacement) that plot within the chondritic range, indicating that their mantle sources evolved with time-integrated near-chondritic Pt/Os ratios. The other four komatiite systems have non-chondritic initial μ^{186}Os values and, thus, evolved with either supra-chondritic (the Weltevreden, Kostomuksha, and Lapland systems) or sub-chondritic (the Komati system) time-integrated Pt/Os ratios. Importantly, among the mantle sources with non-chondritic Re-Os and/or Pt-Os systematics, only in the Kostomuksha komatiite source are these isotope systematics coupled, whereas in the others, they are decoupled.

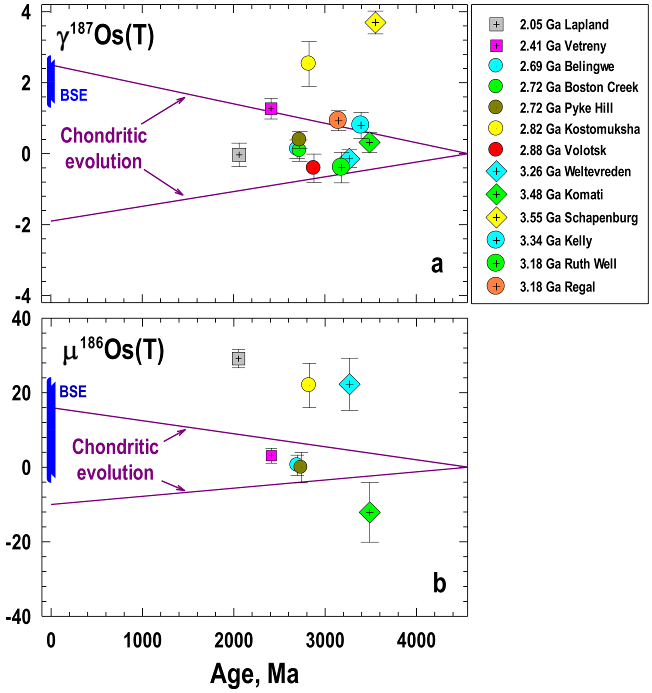

Fig. 2. **(a)** Initial ^{187}Os/^{188}Os, expressed as γ^{187}Os, and **(b)** initial ^{186}Os/^{188}Os, expressed as μ^{186}Os, of Archean komatiite systems studied to date, plotted as a function of their age. The blue bars for the modern BSE estimates represent the 2SD of the mean from Meisel et al. (2001) and Brandon et al. (2006) for (a) and (b), respectively. Data are from: 2.05 Ga Lapland – Puchtel et al. (2020); 2.41 Ga Vetreny – Puchtel et al. (2016b); 2.69 Ga Belingwe and 2.72 Ga Pyke Hill – Puchtel et al. (2009a); 2.72 Ga Boston Creek – Puchtel et al. (2018); 2.82 Ga Kostomuksha – Puchtel et al. (2005); 2.88 Ga Volotsk – Puchtel et al. (2007); 3.48 Ga Komati and 3.26 Ga Weltevreden – Puchtel et al. (2014); 3.55 Ga Schapenburg – Puchtel et al. (2009b, 2016a); 3.34 Ga Kelly and 3.18 Ga Ruth Well and Regal – Puchtel et al. (2022). The data for chondritic meteorites from Walker et al. (2002), Horan et al. (2003), Brandon et al. (2005, 2006), and Fischer-Gödde et al. (2010) are plotted as an envelope enclosed between the slanting purple lines and correspond to the entire range of calculated modern γ^{187}Os and μ^{186}Os values projected back to the Solar System initial ^{187}Os/^{188}Os and ^{186}Os/^{188}Os ratios. All uncertainties are 2SD of the mean.

The total HSE abundances in the komatiite mantle sources have been calculated using the bootstrap method of Puchtel et al. (2004b) that was refined in subsequent studies (*e.g.*, Puchtel et al., 2020, 2022). This method combines the ^{186,187}Os isotopic and HSE abundance data for a suite of komatiitic lavas derived from a common primary magma and related by fractional crystallization of olivine after lava emplacement. The details of the analytical protocol used in the method of Puchtel et al. (2004b) are provided in the ***Electronic Supplement***.

The total HSE abundances in the sources of the komatiite systems considered in this review, calculated as per cent of those in the estimates of the modern BSE of Becker et al. (2006), are presented in Table 2 and plotted as a function of their age in Fig. 3. The calculated total HSE abundances range from ~30% in the 3.55 Ga Schapenburg and 3.53 Ga Coonterunah systems to ~120% in the 2.05 Ga Lapland system. Overall, the entire dataset, except for the obvious outliers (*e.g.*, the 2.72 Ga Boston Creek, 2.69 Ga Belingwe, and 2.41 Ga Vetreny systems), exhibits a broad trend of increasing HSE abundances in the komatiite mantle sources with time. This trend is generally consistent with that defined by the much more scattered data of Maier et al. (2009).

In the following sections, the data reviewed in Section 5 will be discussed in light of the possible mechanisms responsible for creating

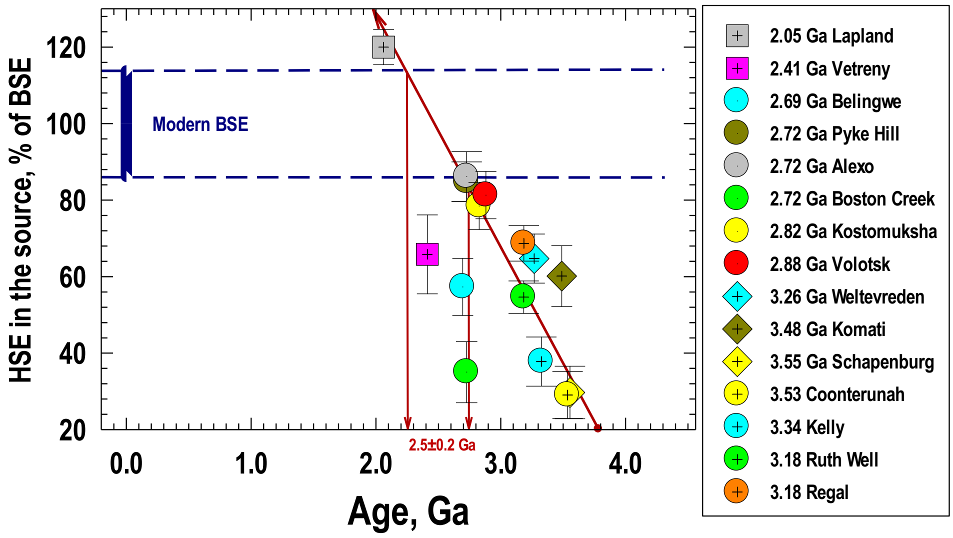

Fig. 3. Calculated total HSE abundances in the sources of Archean and Paleoproterozoic komatiite systems plotted as *per cent* of those in estimates of the modern BSE of Becker et al. (2006). The blue dashed lines correspond to the range for the BSE estimates from Becker et al. (2006). The dark-red arrow represents the regression line through the data. The dark-red vertical arrows represent the projections to the x-axis from the intersections of the regression line with the range for the BSE estimate, thus, illustrating the uncertainties on the average time of homogenization of late accreted materials within the mantle (2.5±0.2 Ga). Data are from: 2.05 Ga Lapland – Puchtel et al. (2020); 2.41 Ga Vetreny Belt – Puchtel et al. (2016b); 2.69 Ga Belingwe – Puchtel et al. (2009a); 2.72 Ga Pyke Hill and Alexo – Puchtel et al. (2004b, 2009a); 2.72 Ga Boston Creek – Puchtel et al. (2018); 2.82 Ga Kostomuksha – Puchtel and Humayun (2005); 2.88 Ga Volotsk – Puchtel et al. (2007); 3.26 Ga Weltevreden and 3.48 Ga Komati – Puchtel et al. (2014); 3.55 Ga Schapenburg – Puchtel et al. (2009b, 2016a); 3.53 Ga Coonterunah, 3.34 Ga Kelly, and 3.18 Ga Ruth Well and Regal – Puchtel et al. (2022). Uncertainties are 2SD. The data reveal a broad trend of increasing HSE abundances in komatiite mantle sources over geological time. All uncertainties are 2SD of the mean. See text for additional details and the ***Electronic Supplement*** for the algorithm used to estimate the HSE abundances in the sources of the komatiite systems.

the early chemical and isotopic heterogeneities in the mantle.

6. Mechanisms for creating early mantle heterogeneities

6.1. Primordial differentiation of the mantle

Crystallization of a primordial magma ocean(s) is one possible mechanism for generating early chemical and isotopic heterogeneities in the mantle (*e.g.*, Boyet et al., 2003, 2021; Boyet and Carlson, 2005, 2006; Caro et al., 2005, 2017; Brown et al., 2014; Puchtel et al., 2016a; Byerly et al., 2017; Morino et al., 2017). Periodic magma oceans are likely a direct consequence of planetary growth due to gravitational energy release from core formation and high-energy collisions during final stages of accretion (*e.g.,* Tonks and Melosh, 1993; Bottke et al., 2010; Rubie et al., 2011). Crystallization of a magma ocean results in stratification controlled by fractionation of mineral assemblages, the composition of which depends on the depth of the magma ocean and the composition of the melted domain. Some studies have argued for occasional, near-complete melting of the silicate Earth, such as may have occurred during the putative giant impact that led to formation of the Moon (Rubie et al., 2011; Canup, 2012; Elkins-Tanton, 2012; Young et al., 2016). The pressures and temperatures near the bottom of such a magma ocean would have stabilized bridgmanite (Mg-perovskite) and Ca-perovskite (Kato et al., 1988; Abe, 1997; Walter et al., 2004). Because most trace elements are variably compatible in Ca-perovskite, with the degree of compatibility decreasing in the order Lu>Hf>Sm>Nd (Corgne et al., 2005), the presence of Ca-perovskite in the fractionating assemblage would result in stronger fractionation of Lu/Hf relative to Sm/Nd than that observed under upper mantle conditions. Over time, this would result in Nd-Hf isotopic decoupling in the mantle domains derived from magma ocean differentiation products, relative to the coupling of these two isotope systems observed in the sources of modern MORB and most OIB, which together define the modern Nd-Hf mantle array, or terrestrial evolution curve (e.g., Salters and White, 1998).

The Nd-Hf mantle array owes its origin to the coupled, or congruent, Nd-Hf isotope systematics of most terrestrial rocks that arise from similar partitioning behavior of the parent (^{147}Sm, ^{176}Lu) and daughter (^{143}Nd, ^{176}Hf) isotopes of the Sm-Nd and Lu-Hf systems during upper mantle differentiation and crust-forming processes (*e.g.,* Patchett et al., 1981; Salters and White, 1998; Vervoort and Blichert-Toft, 1999; Vervoort et al., 1999, 2000). During mantle melting, both parent isotopes are less incompatible with the melt fraction than the daughter isotopes, which results in higher Sm/Nd and Lu/Hf ratios in the melting residue compared to the melt; over time, the residual mantle evolves to more radiogenic Nd and Hf isotopic compositions than the extracted melts. Both isotope systems are lithophile, refractory, insensitive to redox conditions, and largely immobile during alteration and metamorphism. These properties make them useful for investigating the interplay between the formation and recycling of oceanic and continental crust in driving the geochemical evolution of the mantle.

The decoupling of the Nd and Hf isotope systematics (and, thus, deviation from the terrestrial Nd-Hf array) in the early Archean komatiite-basalt systems from the Kaapvaal Craton, such as Schapenburg, Weltevreden, and Komati, have been interpreted to reflect the involvement of primordial magma ocean processes.

Based on the combined ^{142,143}Nd and ^{176}Hf systematics, Puchtel et al. (2013) developed a model of formation of the mantle silicate reservoirs that gave rise to the Komati and Weltevreden komatiites *via* crystallization of a primordial magma ocean. According to their model, during magma ocean differentiation, the lower three quarters of the magma column (from depths of ~2900 to ~700 km) were largely dominated by bridgmanite, with subordinate amounts of ferropericlase and Ca-perovskite, Ca-Pv (Trønnes and Frost, 2002; Ito et al., 2004; Caro et al., 2005; Elkins-Tanton, 2008). Puchtel et al. (2013) used an equilibrium crystallization model based on the high-pressure and -temperature partitioning studies of Corgne and Wood (2002, 2004), Corgne et al. (2005), Liebske et al. (2005), and Walter et al. (2004), and assumed a completely molten mantle with a composition corresponding to that of the early depleted reservoir (EDR) of Boyet and Carlson (2006) that crystallized within the first 150 Ma of the Solar System history, i.e., by 4400 Ma.

Since the study of Puchtel et al. (2013), the EDR model of Boyet and Carlson (2006) has been proven untenable. This model was based on the data available at the time that showed that the accessible Earth has a greater ^{142}Nd/^{144}Nd ratio than chondrites (Carlson et al., 2007). This ^{142}Nd difference required a higher-than-chondritic Sm/Nd ratio for the accessible Earth, which must have been acquired during global silicate differentiation within the first 30 million years of Solar System formation (Boyet and Carlson, 2006) and implied the formation of a complementary reservoir with a lower-than-chondritic Sm/Nd ratio that is either hidden in the deep Earth, or was lost to space by impact erosion (Caro et al., 2008). However, Burkhardt et al. (2016) showed that, compared to chondrites, Earth's building blocks were enriched in ^{142}Nd that was produced by the s-process of nucleosynthesis, which leads to higher ^{142}Nd/^{144}Nd ratios. After these authors corrected for this effect, the ^{142}Nd composition of chondrites and the accessible Earth were shown to be indistinguishable. The results of Burkhardt et al. (2016), therefore, obviate the need for a hidden-reservoir or ^{142}Nd-super-chondritic Earth models and imply a chondritic Sm/Nd ratio for the BSE.

In view of the new data of Burkhardt et al. (2016), we have modified the model of Puchtel et al. (2013), as illustrated in Fig. 4; the methodology used in these model calculations are available as an ***Electronic Supplement***. The composition of the primordial magma ocean, unlike in our previous model, is now represented by that of the chondritic uniform reservoir (CHUR).

Fig. 4 shows the time-integrated ^{147}Sm/^{144}Nd and ^{176}Lu/^{177}Hf ratios in the sources of the Komati and Weltevreden komatiite systems formed as a result of the 4400 Ma magma ocean differentiation and crystallization event specified above, depending on the relative proportions of fractionating bridgmanite and Ca-Pv. The upper panel of the diagram represents aggregate compositions of the magma ocean cumulates, while the lower panel represents the compositions of the residual liquids. As mentioned in the previous model, the contrasting partitioning behavior of Lu and Hf between bridgmanite and Ca-Pv results in differentiation trends that are highly affected by the relative proportions of these two phases. According to the new model, the Komati and Weltevreden mantle domains represent solidification products of a bridgmanite-Ca-Pv cumulate that was derived from ~20% and 12% accumulation of a bridgmanite:Ca-Pv assemblage in the proportions of 93:7 and 80:20, respectively. These proportions and the degrees of magma ocean crystallization are within the range of those envisaged for lower mantle conditions during the Hadean (*e.g.*, Caro et al., 2005). If the modified model of Puchtel et al. (2013) presented here is correct, the mantle plumes that gave rise to the Komati and Weltevreden komatiites must have originated in the lower mantle (Table 1).

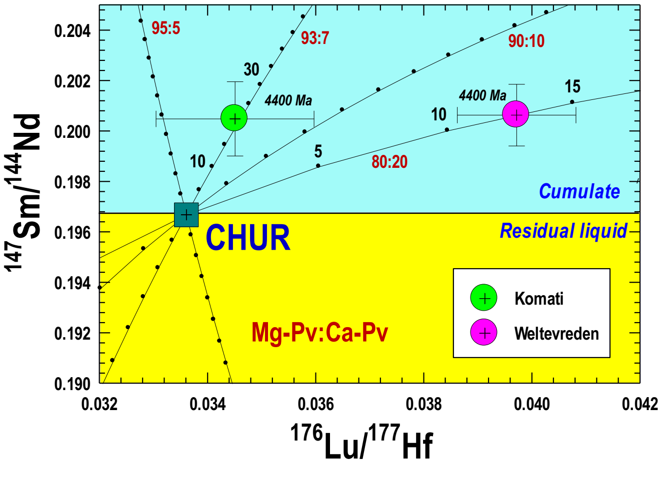

Fig. 4. Evolution of the time-integrated ^{147}Sm/^{144}Nd and ^{176}Lu/^{177}Hf in the calculated sources of the Komati and Weltevreden komatiite systems formed during crystallization of a primordial magma ocean. The differentiation trends (shown by tick marks in percentage) depend on the relative proportions of the fractionating lower mantle mineral phases, *i.e.*, bridgmanite (Mg-Pv) and Ca-Pv. The composition of the magma ocean prior to onset of crystallization is represented by that of the CHUR. The upper part of the panel represents aggregate compositions of magma ocean cumulates, while the lower part of the panel represents compositions of residual liquids after removal of the respective amounts of cumulate bridgmanite and Ca-Pv. All uncertainties are 2SD of the mean. See text for additional details of the model and the ***Electronic Supplement*** for the algorithm used in the calculations.

Boyet et al. (2021) obtained a slightly negative average μ^{142}Nd value of -4.0 ± 4.1 for a set of Komati drill core samples. As noted above, that study combined their ^{142}Nd results with the ^{143}Nd and ^{176}Hf data of Blichert-Toft et al. (2015) for clinopyroxene separates from the same rocks. In order to explain the negative μ^{142}Nd and ε^{143}Nd values and the corresponding positive ε^{176}Hf value, Boyet et al. (2021) proposed a four-stage model for the formation of these lavas, whereby the negative μ^{142}Nd value and low Hf/Sm ratios developed during the crystallization of a deep magma ocean shortly after Earth accretion. The material that ultimately became the source of the komatiites was a residual liquid produced by 50% crystallization of a bridgmanite/ferropericlase/Ca-Pv mineral assemblage in the proportions 79:16:5, which resulted in decoupling of the Nd and Hf isotope systematics. Thus, the model of Boyet et al. (2021) also supports a lower mantle origin for the plume that gave rise to the Komati komatiites.

Metal-silicate fractionation processes operating at the high temperatures and pressures during the first ~60 Ma of Solar System history at the base of an early transient magma ocean, or in a partially molten zone at or near the core-mantle boundary (Labrosse et al., 2007), while ^{182}Hf was still extant, have been argued to be capable of generating coupled ^{182}W and ^{186,187}Os heterogeneities in the mantle (Touboul et al., 2012). To explain the enriched ^{182}W and $^{186,\,187}$Os compositions of the Kostomuksha komatiite system, Touboul et al. (2012) envisioned a lower mantle magma ocean reservoir, where silicate melt could potentially equilibrate with metal that represented either the growing core or the metal passing through the molten region on its way to the core. This model is based on experimental data of substantially reduced metal-silicate partitioning for Re and Pt, relative to Os, at high temperatures and pressures (Righter and Drake, 1997; Cottrell and Walker, 2006; Fortenfant et al., 2003; Yokoyama et al., 2009; Brenan and McDonough, 2009), and on the more siderophile behavior of W under the somewhat more reducing conditions that likely existed in the lower mantle during core formation compared to the present-day upper mantle (Wade and Wood, 2005). The model of Touboul et al. (2012) requires the long-term survival of some portion of the mantle in which HSE and MSE were set by high-temperature and -pressure metal-silicate partitioning under reducing conditions. In order to achieve the $^{186,\,187}$Os and ^{182}W isotopic and elemental characteristics of the Kostomuksha komatiite source, Touboul et al. (2012) envisioned a mantle plume tapping this reservoir and mixing material from it with overlying mantle characterized by Os isotopic compositions and HSE concentrations similar to those in estimates for the BSE of Meisel et al. (2001) and Becker et al. (2006), in the proportions of ~1:1 (Fig. 5). If the model of Touboul et al. (2012) is correct, it implies that the plume, which gave rise to the Kostomuksha komatiites, originated in the lowermost mantle.

Isotopic heterogeneities involving the HSE-based isotopic systems have also been argued to be related to primordial magma ocean crystallization processes by Puchtel et al. (2014) in their study of the HSE abundances and $^{186,\,187}$Os compositions of the Komati and Weltevreden komatiite systems considered above. These authors used the experimental partitioning data of Borisov and Palme (1997) and Mallmann and O'Neill (2007) implying that under the highly reducing conditions that may have existed during crystallization of a primordial magma ocean immediately following the main stage of core formation (Frost et al., 2008), solubility of Pt in silicate melts, unlike the other HSE, may have been low and Pt, hence, would have had a strong tendency to form Pt-Fe alloys. Fractionation and subsequent heterogeneous dispersal of Pt-Fe alloys within the mantle could have resulted in the formation of both Pt-enriched and -depleted domains. These would then have evolved with supra- and sub-chondritic Pt/Os ratios, respectively, which over time would have resulted in the decoupling of the ^{186}Os and ^{187}Os systems in these domains (Puchtel et al., 2014).

A model of silicate-silicate fractionation during primordial mantle magma ocean crystallization, involving early removal of bridgmanite and Ca-Pv, was also proposed by Puchtel et al. (2016a) to explain the

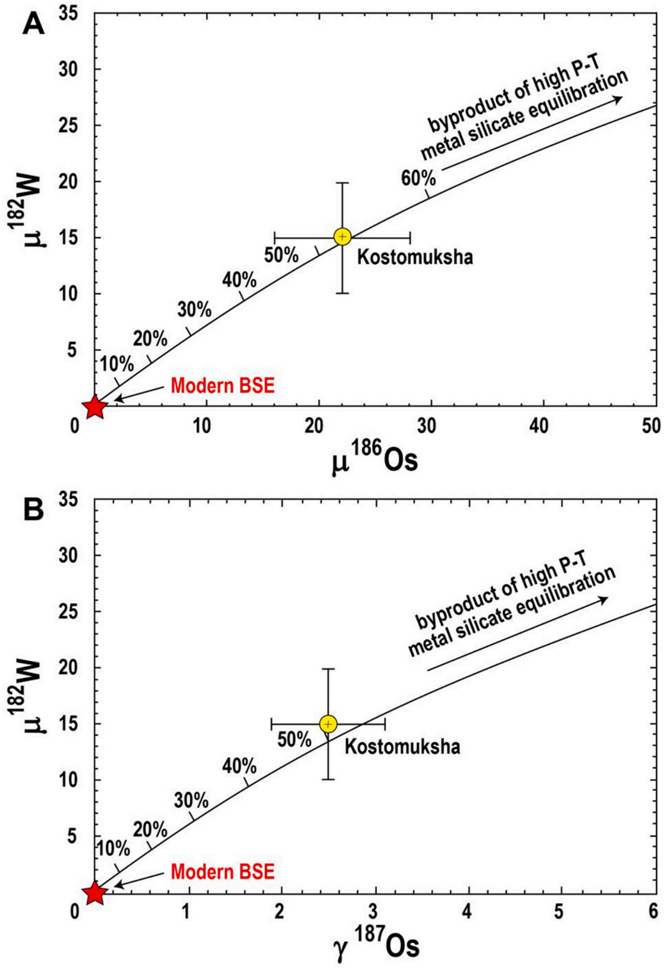

Fig. 5. Values of μ^{182}W versus (A) μ^{186}Os and (B) γ^{187}Os in the Kostomuksha komatiites illustrating mixing between the modern BSE and a mantle reservoir preserved from an early magma ocean crystallization event. The Re/Os, Pt/Os, and Hf/W ratios were established by high-pressure and -temperature metal-silicate equilibrium, resulting in ^{187,186}Os and ^{182}W enrichments at 2.82 Ga (Touboul et al., 2012). The coupled ^{186,187}Os and ^{182}W excesses in the source of the Kostomuksha komatiites (yellow circle) are explained by a ~50% contribution from the isotopically enriched reservoir to the modern BSE. All uncertainties are 2SD of the mean. See text for additional details.

coupled ^{182}W and ^{142}Nd, and decoupled ^{143}Nd and ^{176}Hf isotope systematics of the Schapenburg komatiite source. In their model, the authors recognized that crystal-liquid fractionation in a purely silicate system of a global primordial magma ocean would lead to high Hf/W, Sm/Nd, and Lu/Hf in early-formed cumulates and low Hf/W, Sm/Nd, and Lu/Hf in the residual liquid. If these fractionation processes occurred while ^{182}Hf and ^{146}Sm were still extant, the residual silicate liquid would have developed a coupled deficit in ^{182}W and ^{142}Nd, compared to the ambient mantle, which is what has been observed in the 3.55 Ga Schapenburg komatiites. If the model of Puchtel et al. (2016a) is applicable, it places the mantle domain that served as the sources for the Schapenburg mantle plume in the lowermost mantle.

6.2. Late accretion

The term “late veneer” was first introduced by Turekian and Clark (1969) and later elaborated on by Chou (1978) and Chou et al. (1983) to explain the excess of HSE abundances in the terrestrial mantle compared to what would otherwise be expected after core formation on the basis of the low-pressure and -temperature metal-silicate experimental partitioning data available at the time (*e.g.*, Kimura et al., 1974). Late accretion is defined as the accretion of 0.5-1% (Walker, 2009) of Earth’s mass of a chondritic component after cessation of core formation. In earlier studies, it was assumed that this chondritic component was added to the surface of the Earth in the form of relatively small objects to create a thin layer initially coating the entire planet (thus the term “veneer”). It has also been proposed that a slow downward mixing of this putative thin layer into the mantle was responsible for the apparent trend of increasing HSE abundances in Archean komatiites over time (Maier et al., 2009). Studies by Bottke et al. (2002, 2007), however, have concluded that it is unlikely that late accretion in the form of small objects could have achieved an Earth/Moon late accretionary mass influx ratio of ~1200 required on the basis of the Re-Os isotopic and HSE abundance studies of terrestrial (Meisel et al., 2001; Becker et al., 2006; Fischer-Gödde et al., 2011) and lunar (Walker et al., 2004; Walker, 2014; Day et al., 2007; Day and Walker, 2015) samples. Bottke et al. (2010) proposed that late accretion to Earth was dominated by addition of a few large projectiles, with a mean diameter of ~2000 km, and that HSE were added to the Moon through the accretion of much smaller bodies, ~200 km in diameter. Projectiles with a diameter of 2000 km hitting the Earth likely have been differentiated into HSE-rich cores and HSE-stripped silicate mantles (Marchi et al., 2018). As a result, mantle domains with low HSE abundances and positive ^{182}W anomalies, on the one hand, and high HSE abundances and negative ^{182}W anomalies, on the other hand, would have been generated. In the absence of modern-style plate tectonics prior to ~2.5 Ga (*e.g.*, Brown and Johnson, 2018), these mantle domains would be expected to survive for extended periods of time before eventually becoming homogenized within the mantle *via* wholesale mantle convection.

Heterogeneous distribution of HSE in the early Earth’s mantle has been recognized from ^{186,187}Os and HSE abundance studies of komatiites (*e.g.*, Maier et al., 2009; Puchtel et al., 2004a,b, 2005, 2009a,b, 2014, 2016a,b, 2018, 2020, 2022). As noted in Section 5, available high-precision ^{187}Os data for komatiitic systems worldwide indicate that most komatiite sources were characterized by initial γ^{187}Os values ranging from only −0.1 to +1.3, implying that these komatiitic systems evolved with long-term Re/Os well within the range of chondritic meteorites (Fig. 2a). Only two exceptions have been identified so far, which are the Schapenburg and Kostomuksha komatiite systems. The more limited ^{186}Os dataset indicates a somewhat greater variability outside of the chondritic range, but, nevertheless, suggests that the mantle sources of the late Archean Pyke Hill, Belingwe, and Vetreny komatiite systems evolved with time-integrated Pt/Os within the chondritic range (Fig. 2b). By contrast, the high initial μ^{186}Os and γ^{187}Os values in the mantle source of the Kostomuksha komatiites require long-term suprachondritic Pt/Os and Re/Os ratios. Originally, these coupled ^{186,187}Os enrichments were interpreted to be the result of core-mantle interaction processes (Puchtel et al., 2005). However, the ^{182}W data obtained by Touboul et al. (2012) for these komatiites rendered this interpretation implausible and these authors, instead, proposed that the combined ^{186,187}Os and ^{182}W systematics were the result of metal-silicate fractionation in a primordial magma ocean, as discussed earlier. Additional contrasts are the Komati and Weltevreden (Puchtel et al., 2014) and the Lapland (Puchtel et al., 2020) komatiite systems, which evolved with non-chondritic time-integrated Pt/Os ratios and chondritic time-integrated Re/Os ratios, thereby displaying decoupling of the ^{186}Os and ^{187}Os systematics. For the Komati and Weltevreden komatiite systems, this decoupled behavior has been interpreted to be the result of fractionation of Pt-Fe alloys in a primordial magma ocean during the first 150 Ma of Earth history, followed by slow homogenization of the crystallized post-magma ocean mantle domains characterized by fractionated Pt/Os ratios (Puchtel et al., 2014). For the Lapland komatiite system, derivation from a mantle domain characterized by an excess of late accreted, differentiated planetesimal core metal, the so-called “grainy” late accretion (Walker, 2016), were considered to be one of the two plausible models for explaining the decoupled ^{186}Os and ^{187}Os systematics (Puchtel et al., 2020).

On the basis of variable Pt and Ru contents in komatiites of various ages, Maier et al. (2009) argued for a gradual increase in HSE abundances in the presumed deep mantle sources of komatiites between ~3.5 and ~2.9 Ga due to slow downward mixing of a "late veneer" of chondritic materials. However, the ^{186,187}Os and ^{182}W isotopic and HSE abundance studies of Puchtel et al. (2020, 2022, and references therein) of the best preserved early Archean to early Proterozoic komatiite systems worldwide revealed a somewhat more complex picture. As attested to by the plot of the calculated total HSE abundances in the sources of these komatiite systems as per cent of those in the estimates for the modern BSE of Becker et al. (2006) versus age (Fig. 3), this trend has been argued unlikely to be the result of simple "slow downward mixing of a late veneer of chondritic materials", although a broad trend of increasing HSE abundances in komatiite sources over time is apparent (*e.g.*, Puchtel et al., 2016a, 2018, 2020, 2022). The argument is two-fold. First, as is evident from Fig. 3, the total HSE abundances in the sources of some late Archean komatiite systems were even lower than those in some early Archean komatiite systems. Second, for some of the komatiite systems considered here, *e.g.*, the Schapenburg and Kostomuksha komatiites, the calculated total HSE abundances were shown to be inconsistent with the proportion of late accreted materials estimated to have been added to their sources based on the ^{186,187}Os and ^{182}W data (Touboul et al., 2012; Puchtel et al., 2016a).

These observations are illustrated in Fig. 6, where the μ^{182}W values of komatiite systems are plotted against the calculated total HSE abundances in their mantle sources normalized to those in the estimates for the modern BSE of Becker et al. (2006). This proportion corresponds to the fraction of the total HSE budget of the modern BSE added during late accretion, assuming an essentially HSE-free BSE immediately following core formation. According to this model, the HSE budgets, taking into account their respective uncertainties, of those komatiitic systems that plot within the segment constrained by the blue lines in Fig. 6, are consistent with having been established *via* addition of late accreted materials to their mantle source regions. By contrast, the HSE budgets of the komatiite systems that plot outside this segment are presumed to have been affected by additional primordial processes, such as metal-silicate (*e.g.*, the Kostomuksha komatiites: Touboul et al., 2012) or silicate-silicate (*e.g.*, the Schapenburg komatiites: Puchtel et al., 2016a) fractionation in a primordial magma ocean within the first 60 Ma of Solar System history. Furthermore, the combined ^{187,186}Os-^{182}W and HSE abundance data for the Lapland komatiite system (Fig. 6) are consistent with involvement of fractionated metal derived from cores of differentiated planetesimals during late accretion processes and formation of Os-W isotope and HSE abundance heterogeneities in the early mantle (Puchtel et al., 2020).

It has been argued that the impactors that created the largest impact basins on the Moon, Mars, and presumably also the Earth, were hundreds of km in diameter (Ryder, 2002; Strom et al., 2005; Bottke et al., 2010) and possibly dominated by differentiated planetesimals. Impacts of such bodies would be capable of generating large ^{182}W and HSE anomalies in portions of the mantle as a result of such "grainy" late accretion (Walker, 2016; Marchi et al., 2018, 2020). Cores of differentiated planetesimals would have up to two orders of magnitude higher W abundances, and up to 350 ppm less radiogenic ^{182}W/^{184}W, than the modern BSE (Kleine et al., 2002, 2004; Schoenberg et al., 2002; Yin et al., 2002). Hence, any mantle domain to which an excess of this material was added would be ^{182}W-depleted and would also be expected to be enriched in HSE, compared to BSE, as is observed for the Lapland komatiite system (Puchtel et al., 2020). On the other hand, the mantle domain to which less of a late accretionary HSE component was added, *e.g.*, in the form of the HSE-stripped silicate mantles of differentiated planetesimals, would be ^{182}W-enriched, compared to those mantle domains to which a full HSE complement of late accretionary material was added, and would also be depleted in HSE relative to BSE. A typical example of a komatiite system derived from such a mantle domain is the Boston Creek system (Puchtel et al., 2018).

Using the data for the komatiite systems, for which late accretion has been argued to be the main cause for the observed ^{182}W versus source HSE abundance relationships (Fig. 6), and assuming that the ^{182}W excesses were due entirely to a deficit of late accreted materials in their mantle sources, Puchtel et al. (2022) estimated μ^{182}W of the pre-late accretionary BSE to be +17±7 (Fig. 6). This estimate is consistent with the ^{182}W excess in the pre-late accretion BSE of +18±9 ppm obtained by Kleine and Walker (2017) using an independent approach and to the estimates for the ^{182}W composition of the pre-late accretionary Moon of +25±5 ppm (Kruijer et al., 2015; Touboul et al., 2015; Kruijer and Kleine, 2017). These similarities provide further support to the hypothesis that the Earth and the Moon formed from material with identical W isotopic compositions (Kleine and Walker, 2017), in concert with earlier observations of similarity of O, Si, and Ti isotopic compositions between the Earth and the Moon (*e.g.*, Dauphas et al., 2014), as well as additional evidence that the Moon likely formed mainly from terrestrial, rather than impactor, material.

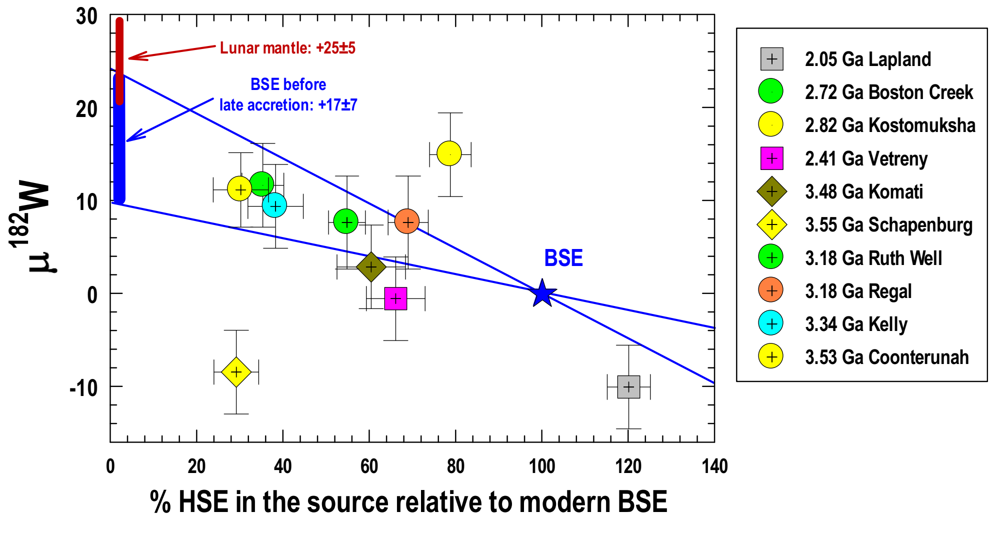

Fig. 6. μ^{182}W (ppm) versus calculated total HSE abundances in the sources of Archean and Paleoproterozoic komatiite-basalt systems studied to date relative to those in the estimates for the present-day BSE of Becker et al. (2006). This proportion corresponds to the fraction of the total HSE budget of the BSE added during late accretion assuming an HSE-free terrestrial mantle prior to late accretion. The average μ^{182}W value for the Moon of +25±5 is from Kruijer et al. (2015) and Touboul et al. (2015). The μ^{182}W of the BSE prior to late accretion is constrained *via Isoplot* regression analysis of the μ^{182}W and HSE compositions of all komatiite-basalt systems, except for those of Kostomuksha and Schapenburg, and the present-day BSE to be +17±7. The W isotopic data and estimates of the HSE contents for the komatiite systems are from Puchtel and Humayun (2005), Touboul et al. (2012), and Puchtel et al. (2014; 2009b, 2016a,b; 2018; 2020; 2022). All uncertainties are 2SD of the mean. See text for additional details.

6.3. Core-mantle boundary processes

Core-mantle exchange is yet another process that may have been responsible for creating ^{182}W and $^{186,\,187}$Os isotope and HSE abundance heterogeneities in the mantle. Originally, the idea was proposed by Walker et al. (1995) based on their studies of the Re, Pt, and Os partitioning behavior in group IIAB magmatic iron meteorites. Walker et al. (1995) noted that during magmatic differentiation, solid metal – liquid metal partition coefficients decrease in the order $D_{Os}>D_{Re}>D_{Pt}$, so that after crystallization of the inner core, the liquid outer core would end up with supra-chondritic Re/Os and Pt/Os and, over time, would develop coupled $^{186,\,187}$Os enrichments. Walker et al. (1997) observed a coupled radiogenic $^{186,\,187}$Os signature in the Noril'sk sulfide ores, which they interpreted as having originated from interaction of the starting 251 Ma Siberian superplume (*e.g.*, Campbell, 2007) with the liquid outer core metal at the CMB.

The concept of core-mantle interaction was further elaborated upon by Brandon et al. (1998, 1999, 2003) and Puchtel et al. (2005) in their studies of plume-derived ocean island basalts and komatiites. These authors proposed that the type of correlation between the initial μ^{186}Os and γ^{187}Os values observed in plume-derived Hawaiian picrites and Gorgona Island and Kostomuksha komatiites is unique to mixtures with fractionated liquid outer core metal (Pt/Re ~100), whereas common crustal materials have Pt/Re <30.

The major drawback of the original core-mantle interaction model stems from the fact that the onset of inner core crystallization is poorly constrained, ranging from <1.0 to 3.5 Ga given the uncertainties in estimates of present-day heat flux at the CMB, which vary from 3 to 10 TW (see review in Nakagawa, 2020, and references therein), as well as currently insufficient knowledge of partitioning behavior of radioactive elements (*e.g.*, K) under the CMB conditions. Another issue concerns the fact that the core-mantle interaction model of Walker et al. (1995) and Brandon et al. (1998, 1999) calls for physical addition of ~1% of the outer core liquid metal to the silicate lower mantle. Because the liquid outer core has up to three orders of magnitude higher HSE abundances compared to the mantle, not only the $^{186,\,187}$Os composition of the resulting hybrid mantle source would be dominated by that of the outer core, but this source would also have had an order of magnitude higher HSE abundances compared to those in the BSE. Most OIB, including Hawaiian picrites, are sulfur-saturated melts, and likely to have lost a significant part of their HSE inventory to either immiscible sulfide liquid fractionation, or to retaining residual sulfide in their melting source regions (*e.g.*, Shirey and Walker, 1998; Bennett et al., 2000; Jamais et al., 2008; Ireland et al., 2009). Such loss of HSE during magma generation and ascent would not be expected to be the case for komatiites, however, because komatiites are strongly sulfur-undersaturated magmas and, therefore, reliably record the HSE abundances in their mantle source regions upon emplacement. Yet, those komatiites for which input from the outer core has been advocated to explain their coupled ^{186,187}Os enrichments, *e.g.*, Gorgona Island (Brandon et al., 2003) and Kostomuksha (Puchtel et al., 2005) komatiites, have calculated HSE abundances in their mantle source regions similar to those in estimates for the modern BSE.

To reconcile the core-mantle interaction model based on the ^{187}Os (Puchtel et al., 2001) and HSE abundance data for the Kostomuksha komatiites with this apparent inconsistency, Puchtel and Humayun (2000) proposed a mechanism of core-mantle interaction *via* isotopic exchange at the core-mantle interface, without any significant mass transfer from the core to the mantle. This idea has been further developed by Humayun (2011). The mechanism of core-mantle interaction of Humayun (2011) requires the outer core liquid to be trapped in a cumulate pile of Fe-rich, non-metallic precipitates (FeO, FeS, Fe_3Si) at the top of the core, then undergo fractional crystallization by precipitating solid metal grains and leaving behind the residual metallic liquid. The residual liquid is then incorporated into the base of the mantle, where it subsequently may be entrained by mantle plumes.

Based on the discovery of negative μ^{182}W values in some modern OIB, Mundl et al. (2017), Rizo et al. (2019), and Mundl-Petermeier et al. (2019, 2020) have also argued for some form of core-mantle exchange/equilibration in order to transfer the inferred negative μ^{182}W value of the core of –220 to plumes rising from the CMB. Although the ^{186,187}Os and ^{182}W data obtained on the same samples are still limited, all Hawaiian lavas with negative μ^{182}W (ranging between –7.8 and –20.2) are also characterized by positive μ^{186}Os (ranging between +18.6 and +62.8) and positive γ^{187}Os (ranging between +2.0 and +7.2). Furthermore, Puchtel et al. (2020) obtained a negative μ^{182}W value of –10 for the Lapland komatiites, which is within the range of the μ^{182}W values obtained for Hawaii, and proposed that Lapland komatiites could be early Proterozoic equivalents of Hawaiian picrites. A core-mantle interaction process, as put forward by Puchtel et al. (2020), would be expected to have decreased the ^{182}W value in the Lapland komatiite source relative to the ambient mantle, and also have increased the HSE abundances in this source over ambient mantle levels, which is consistent with the observations (Fig. 6). That study further proposed that if the residual metal in the model of Humayun (2011) had a composition similar to that of fractionated iron meteorites, its entrainment into the mantle plume that gave rise to the Lapland komatiites could explain the decoupled ^{186,187}Os systematics of these komatiites.

6.4. Crustal recycling processes

Yet another important mechanism for creating mantle chemical heterogeneities is recycling of Earth's mantle lithosphere, oceanic crust, and sedimentary layers back into the mantle (*e.g.,* Hofmann and White, 1982; Shirey and Hanson, 1986; Chase and Patchett, 1988; Campbell and Griffiths, 1992; Hart et al., 1992; Carlson, 1994; Roy-Barman and Allègre, 1995; Widom, 1997; Lassiter and Hauri, 1998; Blichert-Toft et al., 1999; Lassiter, 2006). This recycling may occur via subduction – a process by which one tectonic plate moves under another and sinks into the mantle as the plates converge; subduction is the driving force behind modern plate tectonics. The subducted material may age in the mantle for hundreds of millions of years until entrained in mantle plumes. Although there is little agreement on the timing of the onset, or even existence, of modern-style plate tectonics in the Hadean and Archean (*e.g.*, Brown, 2007; Shirey et al., 2008; Gerya, 2014; Sizova et al., 2015; Johnson et al., 2017; Bédard, 2018), several lines of geochemical evidence put forward by Shirey et al. (2008) require that some version of modern-style plate tectonics already operated as far back in Earth history as 3.5 billion years ago, followed by a transition from the stagnant-lid to mobile-lid plate tectonic regimes sometime in the late Archean (O'Neill and Debaille, 2014).

Crustal recycling, *e.g.*, in the form of subduction of pelagic sediments into the mantle, may also cause decoupling of Nd and Hf isotope systematics of lavas from the Nd-Hf terrestrial mantle array, as has been argued to be the case for a suite of drill core Komati komatiite samples (Blichert-Toft et al., 2015). This is due to the fact that the Lu/Hf ratio is more strongly fractionated, relative to the Sm/Nd ratio, in the Earth's sedimentary system (Patchett et al., 1984). This is caused by high resistance to chemical weathering of the mineral zircon, which contains most of the Hf budget of continental crustal rocks. During weathering of continental crustal rocks, they break down into zircon-bearing sandy sediments, with very low Lu/Hf, and fine-grained clay material, with up to three times the chondritic Lu/Hf ratio. During sediment transport via turbidity currents, sandy sediments stay on or near the continent, while the pelagic material is carried out onto the ocean floor, where it may eventually be subducted into the mantle.

7. The Nd-Hf-Os isotope paradox and its implications for early Earth history

As noted above, there is evidence for decoupling between the radiogenic lithophile ^{143}Nd and ^{176}Hf systems in certain komatiites mantle sources. There is also apparent decoupling between these lithophile isotope systems and the highly siderophile ^{187}Os system in some komatiite mantle sources. The majority of the Archean and Proterozoic komatiite systems are characterized by variable, and generally strong, long-term depletions in more incompatible lithophile trace elements relative to less incompatible elements, *e.g.*, Nd versus Sm and Hf versus Lu (Fig. 1), yet they retain chondritic time-integrated Re/Os ratios (Fig. 2). These komatiite mantle sources must have experienced relatively early melt depletion events that fractionated the Sm/Nd and Lu/Hf ratios to supra-chondritic values high enough to bring the ^{143}Nd and ^{176}Hf compositions to the variably positive ε^{143}Nd and ε^{176}Hf values. Since Re is generally moderately to highly incompatible during mantle melting, whereas Os is moderately to highly compatible (*e.g.*, Barnes et al., 1985; Mallmann and O'Neill, 2007), these melt extraction events should have also decreased the Re/Os ratio in the komatiite-basalt mantle sources. This would have resulted in retardation of ^{187}Os ingrowth and, thus, evolution of the sources to variably negative γ^{187}Os values. However, such isotopic relationships are not observed in the global komatiite-basalt record.

Puchtel et al. (2022) named this phenomenon the Nd-Hf-Os isotope paradox, to which Puchtel et al. (2020, 2022) offered a solution by developing a model, whereby the komatiite-basalt mantle sources underwent early (~100 Ma into Solar System history), low-degree ($F =$ 1.5-2.0%) partial melting and melt extraction events, that would have sufficiently fractionated the Sm/Nd and Lu/Hf ratios in the mantle sources, but would have had little effect on the Re/Os ratio due to the significantly lower incompatibility of Re compared to Nd and Hf during low-degrees of partial mantle melting.

Because this depleted reservoir is apparently persistent throughout the Archean and is globally distributed, it requires early formation and subsequent complete isolation of a complementary basaltic crust enriched in incompatible lithophile trace elements. Calculations by Puchtel et al. (2022) indicate that such crust formed as a result of 1.5-2.0% batch melting of a BSE-like mantle would contain 31-27 ppm Nd, 7.1-6.5 ppm Sm, 0.62-0.59 ppm Lu, and 5.2-4.7 ppm Hf, and would have ^{147}Sm/^{144}Nd = 0.140-0.145 and ^{176}Lu/^{177}Hf = 0.0166-0.0174 (compared to 0.1967 and 0.0336 in the BSE, respectively). Based on these estimates of lithophile trace element concentrations in the early crust, the mass of this reservoir must have represented ≤2.0% of the mass of the BSE, which is consistent with this reservoir being the size of the D" layer. The existence of such crust has been previously advocated for, *e.g.*, by Galer and Goldstein (1991). Alternatively, this earliest mafic crust could have served as the source of the oldest tonalite-trondhjemite-granodiorite (TTG) complexes (Carlson et al., 2019), such as those from, *e.g.*, the Nuvvuagittuq TTG complex in Québec (O'Neil et al., 2008, 2016) or the Vodla Block TTG complex in the Fennoscandian Shield (Puchtel et al., 2016b).

The residence time of this early mafic crust in the mantle is difficult to constrain. The available komatiite-basalt record would require its isolation through at least the late Archean, *i.e.*, when the ^{142}Nd anomalies were apparently still present in the mantle (Debaille et al., 2013). However, there is no evidence that this crust has been stored in the mantle until the present day, based on the generally chondritic ^{138}Ce, ^{142,143}Nd, and ^{176}Hf composition estimates for the BSE (Jackson and Carlson, 2012; Horan et al., 2018; Willig and Stracke, 2019; Willig et al., 2020; Hyung and Jacobsen, 2020).

8. Komatiite constraints on early mixing rates of the terrestrial mantle

It has been proposed that the mixing rates of the mantle, or the average time of mantle homogenization, can be evaluated through studies of short-lived radiogenic isotope systematics and HSE abundances in mantle-derived rocks (*e.g.*, Jacobsen and Yu, 2015; Carlson et al., 2019; Hyung and Jacobsen, 2020; Tusch et al., 2021; Puchtel et al., 2022). Isotopic variations, due to the decay of the now extinct ^{146}Sm and ^{182}Hf nuclides, recorded processes in the Earth that fractionated Sm/Nd and Hf/W ratios between different terrestrial reservoirs at the times when these parent nuclides were still extant. When these events occurred during the first ~600 and ~60 Ma of Earth history, respectively, these differentiation processes over time resulted in formation of ^{142}Nd and ^{182}W anomalies in these terrestrial reservoirs. Due to the protracted, violent accretion history of the Earth, accompanied by vigorous convective mixing during the Hadean and Archean eons, these reservoirs and, thus, the isotopic anomalies they hosted, were gradually homogenized within the mantle. Hence, tracing the variations in the magnitude of these isotopic anomalies over geological time can be used to determine the mixing rates of the terrestrial mantle (*e.g.*, Jacobsen and Yu, 2015; Hyung and Jacobsen, 2020).

Early mantle convection models (*e.g.*, Blichert-Toft and Albarède, 1994; Coltice and Schmalzl, 2006) concluded that the mixing rates in the hot Hadean and Archean mantle were 10 times faster than today, and that any large-scale primordial chemical and isotopic heterogeneities in the mantle would have been erased within ~100 Ma of their creation. However, during the past two decades, numerous ^{142}Nd and ^{182}W anomalies have been discovered in the terrestrial mantle-derived rock record (Fig. 7). The largest ^{142}Nd anomalies (μ^{142}Nd up to +20 ppm and down to −20 ppm) have been reported for Eo- to Paleoarchean supracrustal rocks from the Isua Greenstone Belt, Greenland (Boyet et al., 2003; Caro et al., 2006; Bennett et al., 2007; Rizo et al., 2011, 2012, 2013; O'Neil et al., 2016), the Nuvvuagittuq Greenstone Belt, Québec (O'Neil et al., 2008, 2012; Roth et al., 2013), the Acasta Gneiss Complex, Canada (Roth et al., 2014; Reimink et al., 2018), and the Barberton Greenstone Belt, Kaapvaal Craton, South Africa (Puchtel et al., 2016a; Boyet et al., 2021). These isotopic anomalies must have been created before ~4.0 Ga by silicate-silicate differentiation and, thus, have survived for >1.0 Ga, implying much slower mixing rates of the mantle for ^{142}Nd than was predicted by the early mantle convection models. Following these discoveries, more recent mantle convection models argue for complete homogenization of the mantle by the end of the Archean (*e.g.*, Rosas and Korenaga, 2018; Korenaga, 2021). Indeed, only few terrestrial samples with ages between 3.0 and 2.7 Ga have μ^{142}Nd values deviating from the terrestrial standard by more than ±5 ppm, the only known exception being 2.72 Ga tholeiites from the Abitibi Greenstone Belt, Canada (Debaille et al., 2013). Although there is a significant gap in ^{142}Nd data for the mafic-ultramafic rock record between ~2.7 Ga and the present day, it seems that ^{142}Nd anomalies largely disappeared by the end of the Archean (Fig. 7). As a result, on the basis of the now much larger ^{142}Nd record and using a mathematical mantle mixing box model, Hyung and Jacobsen (2020) concluded that the relationships in Fig. 7 are consistent with mantle mixing rates of ~400 Ma that operated since the early Hadean. These authors further argued that such fast mixing rates are consistent with Earth's thermal and chemical evolution having been largely regulated by plate tectonics for most of its history.

Nonetheless, recent studies have shown that some modern OIB (Fig. 7) have ^{142}Nd compositions statistically resolved, albeit marginally, from that of the terrestrial standard (*e.g.*, Horan et al., 2018; Peters et al., 2018), indicating that some ^{142}Nd isotopic signatures dating back to Earth's earliest differentiation events may still be preserved in deepest parts of the modern mantle.

In contrast to the earliest ^{142}Nd record, mostly positive ^{182}W anomalies, of up to ~+20 ppm, have been reported for mafic-ultramafic rocks ranging in age from 4.0 to 2.7 Ga (Fig. 7b). The only exceptions are komatiites from the Schapenburg system (Puchtel et al., 2016a), which have a negative ^{182}W anomaly of –8 ppm. On the other hand, some recent and modern OIB, such as Hawaii, Samoa, Iceland, Galapagos, Heard, Pitcairn (Mundl et al., 2017; Mundl-Petermeier et al., 2019, 2020), and Kerguelen and Reunion (Rizo et al., 2019) are characterized by negative ^{182}W anomalies down to –25 ppm, although the volumetrically dominant signature in OIB is most likely ^{182}W = 0. The very limited data available (Puchtel et al., 2016b, 2020) provide a hint that there may be a transition at ~2.5 Ga from mostly positive μ^{182}W-

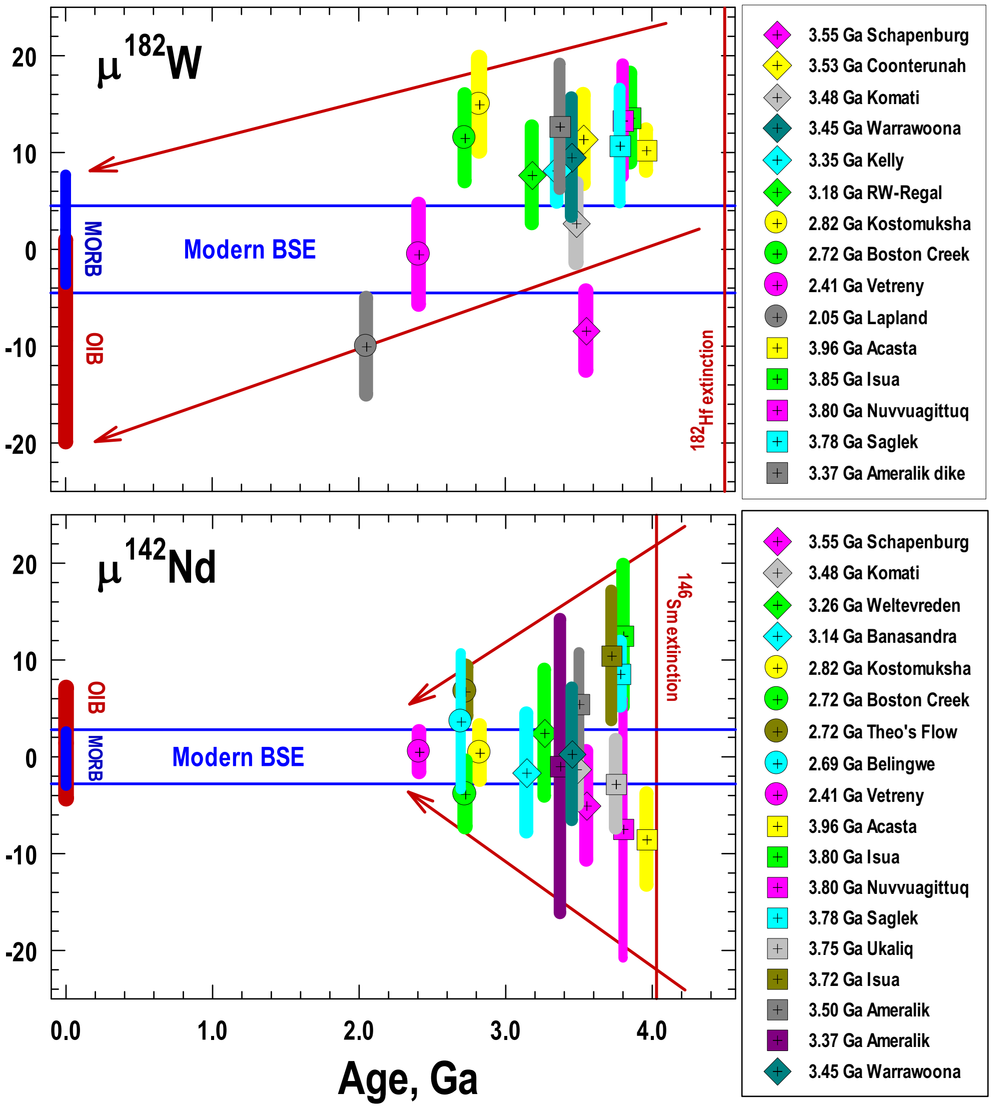

Fig. 7. ^{182}W/^{184}W and ^{142}Nd/^{144}Nd data for the terrestrial mafic-ultramafic rock record obtained to date. The colored bands represent the 2SD uncertainty on the mean μ^{182}W and μ^{142}Nd values for each locality. The dark-red arrows illustrate the change in direction and magnitude of the ^{182}W and ^{142}Nd anomalies. Note the relative scarcity of data for the period between ~2.7 Ga and present day. Data are from: 3.96 Ga Acasta – Roth et al. (2014), Willbold et al. (2015), Reimink et al. (2018); 3.85 Ga Isua – Willbold et al. (2011), Rizo et al. (2013, 2016), Dale et al. (2017), Tusch et al. (2019), Caro et al. (2006), Bennett et al. (2007), Saji et al. (2018); 3.80 Ga Nuvvuagittuq – O'Neil et al. (2012), Touboul et al. (2014); 3.78 Ga Saglek – Liu et al. (2016), Morino et al. (2017); 3.75 Ga Ukaliq – Caro et al. (2017); 3.72 Ga Isua – Rizo et al. (2011, 2016), Tusch et al. (2019), O'Neil et al. (2016); 3.50 Ga Ameralik – Saji et al. (2018); 3.37 Ga Ameralik – Rizo et al. (2012, 2016), Tusch et al. (2019); 3.55 Ga Schapenburg – Puchtel et al. (2016a); 3.53 Ga Coonterunah – Tusch et al. (2021), Puchtel et al. (2022); 3.48 Ga Komati and 3.26 Weltevreden – Touboul et al. (2012), Caro et al. (2006), Puchtel et al. (2013), Schneider et al. (2018); 3.45 Ga Warrawoona – Archer et al. (2019), Rizo et al. (2019), Murphy et al. (2021); 3.35 Ga Kelly – Puchtel et al. (2022); 3.18 Ga Ruth Well and Regal – Archer et al. (2019), Tusch et al. (2021), Puchtel et al. (2022); 3.14 Ga Banasandra – Maya et al. (2017); 2.82 Ga Kostomuksha and 2.69 Ga Belingwe – Touboul et al. (2012), Boyet and Carlson (2006); 2.72 Ga Boston Creek – Puchtel et al. (2018); 2.72 Ga Theo's Flow – Debaille et al. (2013); 2.41 Ga Vetreny Belt – Puchtel et al. (2016b); 2.05 Ga Lapland – Puchtel et al. (2020); modern OIB – Caro et al. (2006), Andreasen et al. (2008), Murphy et al. (2010), Touboul et al. (2012), Mundl et al. (2017), Mundl-Petermeier et al. (2019, 2020), Rizo et al. (2019), Horan et al. (2018), Saji et al. (2018), Peters et al. (2018), Hyung and Jacobsen (2020); modern MORB – Caro et al. (2006), Mundl et al. (2017), Hyung and Jacobsen (2020).

dominated to no-anomaly μ^{182}W-dominated mantle (Fig. 7b). With the relatively young 2.05 Ga Lapland komatiites already registering a negative ^{182}W anomaly of –10 ppm (Puchtel et al., 2020), and some OIB sources registering negative ^{182}W anomalies down to –25 ppm, this transition may indicate the combined effects of the onset of modern-style plate tectonics and core-mantle interaction taking over as the main driving forces controlling the W isoltopic composition of the deep plume mantle sources (*e.g.*, Rizo et al., 2019; Carlson et al., 2019).

The different behavior of the two short-lived isotopic systems in the mantle may be possible to reconcile, when the mechanisms behind the origin of ^{142}Nd and ^{182}W anomalies are considered. Because both Sm and Nd are uniformly strongly lithophile elements under the redox conditions applicable to Earth's formation, ^{142}Nd anomalies are solely the result of primordial silicate-silicate planetary differentiation (*e.g.*, Boyet and Carlson, 2005). No new ^{142}Nd anomalies could have been created in the BSE after ~4.0 Ga, when ^{146}Sm became extinct. In contrast to the ^{146}Sm-^{142}Nd system, Hf is strongly lithophile, while W is moderately siderophile. Hafnium, therefore, can be fractionated from W during metal-silicate differentiation, such as that which occurred during planetary core segregation. During silicate-silicate differentiation, W is more incompatible than Hf, which can result in fractionation of Hf from W in purely silicate systems. Both processes are considered to be capable of creating ^{182}W anomalies within the first 60 Ma of Earth's history, while ^{182}Hf was still extant. The additional processes that are thought to be capable of introducing ^{182}W heterogeneities to the mantle, and to which the ^{142}Nd system was insensitive, were late accretion and core-mantle interaction, as discussed in Section 6. As a result of the combination of all these factors in variable, and generally unconstrained, proportions, the use of the ^{182}Hf-^{182}W isotopic system for tracing the mixing rates of the mantle appears to be of lesser value than the use of the ^{146}Sm-^{142}Nd systematics.

Mantle mixing rates in terms of HSE have been studied *via* tracing the changes in HSE abundances in the mantle over the span of geological time (*e.g.*, Maier et al., 2009; Puchtel et al., 2018, 2020, 2022). Because the lunar highland crust, which was formed at ~4.4 Ga (*e.g.*, Borg et al., 2014), is only negligibly contaminated by meteoritic material (*e.g.*, Day et al., 2010), late accretion must have been largely complete prior to 4.4 Ga, *i.e.*, within the first ~150 Ma of the Solar System history. Puchtel et al. (2022) used the estimated HSE abundances in the sources of the Archean and Proterozoic komatiite systems (Fig. 3) as a function of their ages and *Isoplot* regression analysis to calculate the average time by which the late accreted materials would have been completely homogenized within the mantle, and found 2.5±0.2 Ga. These data require that survival times of the late accreted planetesimals within the mantle, before complete homogenization, were on average 1.9±0.2 Ga (*i.e.,* the time interval between 4.4 and 2.5 Ga), thus constraining the average mixing rates of the terrestrial mantle in terms ofsiderophile element abundances in the Hadean and Archean. This period in time coincides with the timing of the onset of modern-style plate tectonics on Earth, as argued by some (Brown, 2007; Brown and Johnson, 2018), and with the near-complete disappearance of all ^{142}Nd and positive ^{182}W anomalies in the mantle (Carlson et al., 2019; Reimink et al., 2020; Tusch et al., 2021).

It is possible that some inefficient mixing of the terrestrial mantle could be due to early Earth tectonic regimes differing from those of modern-style plate tectonics (O'Neill and Debaille, 2014). A stagnant-lid, or episodic, subduction regime in the Hadean is consistent with the persistence of short-lived isotopic anomalies and compositional heterogeneities, although more recent modeling indicates that such mantle heterogeneities can survive for billions of years even under a mobile-lid tectonic regime (Foley and Rizo, 2017).

9. The diverse nature of komatiite sources reflects on the complexity of the terrestrial mantle

As is evident from the chemical and isotopic data summarized in Tables 1 and 2 and discussed throughout this review, komatiite mantle sources were characterized by extreme diversity throughout the Archean and early Proterozoic in terms of both trace- and HSE abundances and radiogenic isotope systematics. Early Archean komatiites were likely derived from lower mantle domains that were created very early in Earth history as a result of deep-seated magma ocean crystallization processes. These mantle domains were characterized by highly variable, and often strong, long-term depletions in the highly incompatible lithophile trace elements, and generally large deficits in the late accreted component, as attested to by their HSE abundance and ^{182}W systematics.

The late Archean and Proterozoic komatiites show evidence in their mantle sources for limited variability of long-term depletions in highly incompatible lithophile trace elements as a result of prior melt extractions. With the exception of the Kostomuksha and possibly Lapland systems, these komatiites were derived from mantle plumes that originated in the upper mantle, most likely in the MTZ. These komatiite sources were characterized by smaller deficits to excesses in the late accreted component, as testified to by their HSE abundance and ^{182}W systematics.

Finally, our compliation of the geochemical data relevant to the mantle sources of Archean and early Proterozoic komatiites reveals that none of the projected sources were similar in composition to estimates for the BSE. The komatiite systems considered here, which span wide geographical and temporal distributions, further demonstrate that no single petrogenetic model can account for all the diverse chemical compositions of komatiites.

10. Conclusions

Komatiites, due to their unique properties and, with a few exceptions, very old ages, are among the best samples to constrain the evolution of the chemical composition of the early Earth's mantle. Isotopic and elemental signatures created in early-formed silicate reservoirs *via* radioactive decay of short- and long-lived nuclides, including ^{146,147}Sm, ^{176}Lu, ^{182}Hf, ^{187}Re, and ^{190}Pt, have been sampled by komatiitic magmas and preserved in the geological rock record. These signatures have been used here to constrain the nature and timing of formation of these, by now largely vanished, mantle reservoirs.

The komatiites considered in the present review are interpreted to have been derived from anhydrous melting in mantle plumes that were initiated in both the lower and upper mantle, although, in contrast to modern plumes, all evidence for the depths of ancient mantle plume initiation is circumstantial in nature.

The data for the existing 3.6-2.0 Ga komatiite-basalt record provide robust evidence for the presence of remarkably ancient isotopic and chemical heterogeneities in the mantle at that time interval in Earth history. These heterogeneities have been shown here to reflect the combined effects of (i) the co-existence of diverse post-magma ocean silicate domains characterized by variably-fractionated lithophile and siderophile element abundances; (ii) the presence of distinct reservoirs representing mantles and cores of large, differentiated planetesimals delivered to Earth during late accretion; and (iii) isotopic exchange across the core-mantle boundary.

The near-complete disappearance of resolvable ^{142}Nd anomalies and of decoupled ^{143}Nd-^{176}Hf isotopic signatures in the mafic-ultramafic rock record by ~2.5 Ga indicates that the earliest silicate reservoirs, formed as a result of primordial magma ocean crystallization, had been largely destroyed by that time through vigorous, convective mantle mixing, implying mixing rates of the mantle on the order of ~1.5 Ga. The shift from mostly positive ^{182}W offsets in the pre-2.5 Ga mantle sources of mafic-ultramafic lavas to no ^{182}W offsets at ~2.5 Ga, as well as disapperance of HSE abundance anomalies at ~2.5 Ga, may indicate the combined effects of the onset of modern-style plate tectonics and core-mantle interaction that took over as the main driving force of creating ^{182}W isotopic heterogeneities in the mantle.

This review further emphasizes the great compositional complexity of early Archean to early Proterozoic komatiite mantle sources in terms of both lithophile and siderophile element abundances and isotope systematics; apparently, none of these sources were similar in composition to that of the BSE. Obviously, no single petrogenetic model can fully account for the chemical and isotopic diversity of komatiites.

Declaration of Competing Interest

The authors declare that they have no known competing financial interests or personal relationships that could have appeared to influence the work reported in this paper.

Acknowledgements

This work was supported by NSF Petrology and Geochemistry grant EAR 1754186 to ISP. We are grateful to Al Hofmann and Maud Boyet for thorough and constructive reviews of the initial version of this manuscript and to Catherine Chauvel for editorial handling. This work greatly benefitted from close collaborations with Carl Anhaeusser, Nick Arndt, Gary Byerly, Eero Hanski, Al Hofmann, Munir Humayun, Vyacheslav and Victoria Kulikov, Mike Lesher, Marek Locmelis, Euan Nisbet, and Andi Mundl-Petermeier.

Appendix A. Supplementary data

Supplementary data to this article can be found online at https://doi.org/10.1016/j.chemgeo.2022.120776.

References

Abbott, D., 1996. Plumes and hotspots as sources of greenstone belts. Lithos 37 (2-3), 113–127.

Abe, Y., 1997. Thermal and chemical evolution of the terrestrial magma ocean. Phys. Earth Planet. Inter. 100 (1-4), 27–39.

Albarède, F., Blichert-Toft, J., Vervoort, J.D., Gleason, J.D., Rosing, M., 2000. Hf-Nd isotope evidence for a transient dynamic regime in the early terrestrial mantle. Nature 404 (6777), 488–490.

Allègre, C.J., 1982. Genesis of Archaean komatiites in a wet ultramafic subducted plate. In: Arndt, N.T., Nisbet, E.G. (Eds.), Komatiites. George Allen and Unwin, London, pp. 495–500.

Andreasen, R., Sharma, M., Subbarao, K.V., Viladkar, S.G., 2008. Where on Earth is the enriched Hadean reservoir? Earth Planet. Sci. Lett. 266 (1-2), 14–28.

Archer, G.J., Brennecka, G.A., Gleißner, P., Stracke, A., Becker, H., Kleine, T., 2019. Lack of late-accreted material as the origin of ^{182}W excesses in the Archean mantle: Evidence from the Pilbara Craton, Western Australia. Earth Planet. Sci. Lett. 528, 115841.

Arevalo, R., McDonough, W.F., 2008. Tungsten geochemistry and implications for understanding the Earth's interior. Earth Planet. Sci. Lett. 272 (3–4), 656–665.

Armstrong, R.L., 1981. Radiogenic isotopes: the case for crustal recycling on a near-steady-state no-continental-growth. Philos. Trans. R. Soc. Lond. A301, 443–472.

Arndt, N.T., 1977. Ultrabasic magmas and high-degree melting of the mantle. Contrib. Mineral. Petrol. 64 (2), 205–221.

Arndt, N.T., 1994. Archean Komatiites. In: Condie, K.C. (Ed.), Archean Crustal Evolution. Elsevier, Amsterdam, pp. 11–44.

Arndt, N.T., Nisbet, E.G., 1982. Komatiites. Allen and Unwin, London, p. 582.

Arndt, N.T., Naldrett, A.J., Pyke, D.R., 1977. Komatiitic and iron-rich tholeiitic lavas of Munro Township, northeast Ontario. J. Petrol. 18, 319–369.

Arndt, N.T., Ginibre, C., Chauvel, C., Albarède, F., Cheadle, M., Herzberg, C., Jenner, G., Lahaye, Y., 1998. Were komatiites wet? Geology 26 (8), 739–742.

Arndt, N., Bruzak, G., Reischmann, T., 2001. The oldest continental and oceanic plateaus: Geochemistry of basalts and komatiites of the Pilbara Craton, Australia. Geol. Soc. Am. Spec. Pap. 352, 359–387.

Arndt, N.T., Lesher, C.M., Barnes, S.J., 2008. Komatiite. Cambridge University Press, Cambridge, UK, p. 467.

Asafov, E.V., Sobolev, A.V., Gurenko, A.A., Arndt, N.T., Batanova, V.G., Portnyagin, M. V., Garbe-Schönberg, D., Krasheninnikov, S.P., 2018. Belingwe komatiites (2.7 Ga) originate from a plume with moderate water content, as inferred from inclusions in olivine. Chem. Geol. 478, 39–59.

Ballmer, M.D., Schumacher, L., Lekic, V., Thomas, C., Ito, G., 2016. Compositional layering within the large low shear-wave velocity provinces in the lower mantle. Geochem. Geophys. Geosyst. 17 (12), 5056–5077.

Bao, X., Lithgow-Bertelloni, C.R., Jackson, M.G., Romanowicz, B., 2022. On the relative temperatures of Earth's volcanic hotspots and mid-ocean ridges. Science 373 (6576), 57–61.

Barnes, S.J., Van Kranendonk, M.J., 2014. Archean andesites in the east Yilgarn craton, Australia: Products of plume-crust interaction? Lithosphere 6 (2), 80–92.

Barnes, S.-J., Naldrett, A.J., Gorton, M.P., 1985. The origin of the fractionation of platinum-group elements in terrestrial magmas. Chem. Geol. 53 (3-4), 303–323.

Barnes, S.J., Mole, D., Wyche, S., Dering, G., 2016. Komatiites and associated rocks of the Kalgoorlie–Leonora region. In: Geological Survey of Western Australia Record 2016/12, 70 pp.

Becker, H., Horan, M.F., Walker, R.J., Gao, S., Lorand, J.-P., Rudnick, R.L., 2006. Highly siderophile element composition of the Earth's primitive upper mantle: Constraints from new data on peridotite massifs and xenoliths. Geochim. Cosmochim. Acta 70 (17), 4528–4550.

Bédard, J.H., 2018. Stagnant lids and mantle overturns: Implications for Archaean tectonics, magmagenesis, crustal growth, mantle evolution, and the start of plate tectonics. Geosci. Front. 9 (1), 19–49.

Bennett, V.C., Esat, T.M., Norman, M.D., 1996. Two mantle-plume components in Hawaiian picrites inferred from correlated Os-Pb isotopes. Nature 381 (6579), 221–224.

Bennett, V.C., Norman, M.D., Garcia, M.O., 2000. Rhenium and platinum group element abundances correlated with mantle source components in Hawaiian picrites: sulphides in the plume. Earth Planet. Sci. Lett. 183 (3-4), 513–526.

Bennett, V.C., Brandon, A.D., Nutman, A.P., 2007. Coupled ^{142}Nd-^{143}Nd isotopic evidence for Hadean mantle dynamics. Science 318 (5858), 1907–1910.

Bercovici, D., Karato, S., 2003. Whole-mantle convection and the transition-zone water filter. Nature 425 (6953), 39–44.

Berry, A.J., Danyushevsky, L.V., O'Neill, H.S.C., Newville, M., Sutton, S.R., 2008. Oxidation state of iron in komatiitic melt inclusions indicates hot Archaean mantle. Nature 455 (7215), 960–963.

Bickle, M.J., 1982. The magnesium contents of komatiitic liquids. In: Komatiites. George Allen and Unwin, London, pp. 479–494.

Bickle, M.J., 1986. Implications of melting for stabilisation of lithosphere and heat loss in the Archaean. Earth Planet. Sci. Lett. 80 (3-4), 314–324.

Bina, C.R., Helffrich, G., 1994. Phase transition Clapeyron slopes and transition zone seismic discontinuity topography. J. Geophys. Res. 99 (B8), 15853–15860.

Blichert-Toft, J., Albarède, F., 1994. Short-lived chemical heterogeneities in the Archean mantle with implications for mantle convection. Science 263, 1593–1596.

Blichert-Toft, J., Arndt, N.T., 1999. Hf isotope compositions of komatiites. Earth Planet. Sci. Lett. 171 (3), 439–451.

Blichert-Toft, J., Puchtel, I.S., 2010. Depleted mantle sources through time: Evidence from Lu-Hf and Sm-Nd isotope systematics of Archean komatiites. Earth Planet. Sci. Lett. 297 (3-4), 598–606.

Blichert-Toft, J., Frey, F.A., Albarède, F., 1999. Hf isotope evidence for pelagic sediments in the source of Hawaiian basalts. Science 285, 879–882.

Blichert-Toft, J., Arndt, N.T., Wilson, A., Coetzee, G., 2015. Hf and Nd isotope systematics of early Archean komatiites from surface sampling and ICDP drilling in the Barberton Greenstone Belt, South Africa. Am. Mineral. 100, 2396–2411.

Borg, L.E., Gaffney, A.M., Shearer, C.K., 2014. A review of lunar chronology revealing a preponderance of 4.34–4.37 Ga ages. Meteorit. Planet. Sci. 50 (4), 715–732.

Borisov, A., Palme, H., 1997. Experimental determination of the solubility of platinum in silicate melts. Geochim. Cosmochim. Acta 61 (20), 4349–4357.

Bottke, W.F., Morbidelli, A., Jedicke, R., Petit, J.-M., Levison, H.F., Michel, P., Metcalfe, T.S., 2002. Debiased orbital and absolute magnitude distribution of the near-earth objects. Icarus 156 (2), 399–433.

Bottke, W.F., Levison, H.F., Nesvorny, D., Dones, L., 2007. Can planetesimals left over from terrestrial planet formation produce the lunar Late Heavy Bombardment? Icarus 190 (1), 203–223.

Bottke, W.F., Walker, R.J., Day, J.M.D., Nesvorny, D., Elkins-Tanton, L., 2010. Stochastic Late Accretion to Earth, the Moon, and Mars. Science 330 (6010), 1527–1530.

Bouvier, A., Vervoort, J.D., Patchett, P.J., 2008. The Lu-Hf and Sm-Nd isotopic composition of CHUR: Constraints from unequilibrated chondrites and implications for the bulk composition of terrestrial planets. Earth Planet. Sci. Lett. 273 (1-2), 48–57.

Bowring, S.A., Housh, T., 1995. The Earth's early evolution. Science 269 (5230), 1535–1540.

Boyet, M., Carlson, R.W., 2005. ^{142}Nd evidence for early ($>$4.53 Ga) global differentiation of the silicate Earth. Science 309 (5734), 576–581.

Boyet, M., Carlson, R.W., 2006. A new geochemical model for the Earth's mantle inferred from ^{146}Sm-^{142}Nd systematics. Earth Planet. Sci. Lett. 250 (1-2), 254–268.

Boyet, M., Blichert-Toft, J., Rosing, M., Storey, M., Télouk, P., Albarède, F., 2003. ^{142}Nd evidence for early Earth differentiation. Earth Planet. Sci. Lett. 214 (3-4), 427–442.

Boyet, M., Garçon, M., Arndt, N.T., Carlson, R.W., Konc, Z., 2021. Residual liquid from deep magma ocean crystallization in the source of komatiites from the ICDP drill core in the Barberton Greenstone Belt. Geochim. Cosmochim. Acta 304, 141–159.

Brandon, A.D., Walker, R.J., Morgan, J.W., Norman, M.D., Prichard, H.M., 1998. Coupled ^{186}Os and ^{187}Os evidence for core-mantle interaction. Science 280 (5369), 1570–1573.

Brandon, A.D., Norman, M.D., Walker, R.J., Morgan, J.W., 1999. ^{186}Os-^{187}Os systematics of Hawaiian picrites. Earth Planet. Sci. Lett. 174 (1-2), 25–42.

Brandon, A.D., Walker, R.J., Puchtel, I.S., Becker, H., Humayun, M., Revillon, S., 2003. ^{186}Os-^{187}Os systematics of Gorgona Island komatiites: Implications for early growth of the inner core. Earth Planet. Sci. Lett. 206 (3-4), 411–426.

Brandon, A.D., Humayun, M., Puchtel, I.S., Zolensky, M., 2005. Re-Os isotopic systematics and platinum group element composition of the Tagish Lake carbonaceous chondrite. Geochim. Cosmochim. Acta 69 (6), 1619–1631.

Brandon, A.D., Walker, R.J., Puchtel, I.S., 2006. Platinum-osmium isotope evolution of the Earth's mantle: Constraints from chondrites and Os-rich alloys. Geochim. Cosmochim. Acta 70 (8), 2093–2103.

Brenan, J.M., McDonough, W.F., 2009. Core formation and metal-silicate fractionation of osmium and iridium from gold. Nat. Geosci. 2, 798–801.

Brown, M., 2007. Metamorphism, Plate Tectonics, and the Supercontinent Cycle. Earth Sci. Front. 14 (1), 1–18.

Brown, M., Johnson, T., 2018. Secular change in metamorphism and the onset of global plate tectonics. Am. Mineral. 103 (2), 181–196.

Brown, S.M., Elkins-Tanton, L.T., Walker, R.J., 2014. Effects of magma ocean crystallization and overturn on the development of ^{142}Nd and ^{182}W isotopic heterogeneities in the primordial mantle. Earth Planet. Sci. Lett. 408, 319–330.

Burkhardt, C., Borg, L.E., Brennecka, G.A., Shollenberger, Q.R., Dauphas, N., Kleine, T., 2016. A nucleosynthetic origin for the Earth's anomalous ^{142}Nd composition. Nature 537, 394–398.

Byerly, B.L., Kareem, K., Bao, H., Byerly, G.R., 2017. Early Earth mantle heterogeneity revealed by light oxygen isotopes of Archaean komatiites. Nat. Geosci. 10, 871–876.

Campbell, I.H., 2007. Testing the plume theory. Chem. Geol. 241 (3-4), 153–176.

Campbell, I.H., Griffiths, R.W., 1990. Implications of mantle plume structure for the evolution of flood basalts. Earth Planet. Sci. Lett. 99 (1-2), 79–93.

Campbell, I.H., Griffiths, R.W., 1992. The changing nature of mantle hotspots through time: Implications for the chemical evolution of the mantle. J. Geol. 92 (5), 497–523.

Campbell, I.H., Griffiths, R.W., 1993. The evolution of the mantle's chemical structure. Lithos 30 (3), 389–399.

Campbell, I.H., Griffiths, R.W., 2014. Did the formation of D cause the Archaean-Proterozoic transition? Earth Planet. Sci. Lett. 388, 1–8.

Campbell, I.H., Hill, R.I., 1988. A two stage model for the formation of the granite-greenstone terrains of the Kalgoorlie-Norseman area, Western Australia. Earth Planet. Sci. Lett. 90 (1), 11–25.

Campbell, I.H., Griffiths, R.W., Hill, R.I., 1989. Melting in an Archaean mantle plume: head it's basalts, tails it's komatiites. Nature 339 (6227), 697–699.

Canil, D., 1997. Vanadium partitioning and the oxidation state of Archaean komatiite magmas. Nature 389 (6653), 842–845.

Canil, D., 1999. Vanadium partitioning between orthopyroxene, spinel and silicate melt and the redox states of mantle source regions for primary magmas. Geochim. Cosmochim. Acta 63 (3-4), 557–572.

Canil, D., 2002. Vanadium in peridotites, mantle redox and tectonic environments: Archean to present. Earth Planet. Sci. Lett. 195 (1-2), 75–90.

Canil, D., Fedortchouk, Y., 2001. Olivine-liquid partitioning of vanadium and other trace elements, with applications to modern and ancient picrites. Can. Mineral. 39, 319–330.

Canup, R.M., 2012. Forming a moon with an Earth-like composition via a giant impact. Science 338 (6110), 1052–1055.

Carlson, R.W., 1994. Mechanisms of Earth differentiation: consequences for the chemical structure of the mantle. Rev. Geophys. 32 (4), 337–361.

Carlson, R.W., Boyet, M., Horan, M., 2007. Chondrite barium, neodymium, and samarium isotopic heterogeneity and early earth differentiation. Science 316 (5828), 1175–1178.

Carlson, R.W., Boyet, M., O'Neil, J., Rizo, H., Walker, R.J., 2015. Early Differentiation and Its Long-Term Consequences for Earth Evolution. In: The Early Earth. John Wiley & Sons, Inc, Hoboken, New Jersey, pp. 143–172.

Carlson, R.W., Garçon, M., O'Neil, J., Reimink, J., Rizo, H., 2019. The nature of Earth's first crust. Chem. Geol. 530, 119321.

Caro, G., 2011. Early Silicate Earth Differentiation. Annu. Rev. Earth Planet. Sci. 39 (1), 31–58.

Caro, G., Bourdon, B., Birck, J.-L., Moorbath, S., 2003. ^{146}Sm-^{142}Nd evidence from Isua metamorphosed sediments for early differentiation of the Earth's mantle. Nature 423 (6938), 428–432.

Caro, G., Bourdon, B., Wood, B.J., Corgne, A., 2005. Trace-element fractionation in Hadean mantle generated by melt segregation from a magma ocean. Nature 436 (7048), 246–249.

Caro, G., Bourdon, B., Birck, J.-L., Moorbath, S., 2006. High-precision ^{142}Nd/^{144}Nd measurements in terrestrial rocks: Constraints on the early differentiation of the Earth's mantle. Geochim. Cosmochim. Acta 70 (1), 164–191.

Caro, G., Bourdon, B., Halliday, A.N., Quitte, G., 2008. Super-chondritic Sm/Nd ratios in Mars, the Earth and the Moon. Nature 452 (7185), 336–339.

Caro, G., Morino, P., Mojzsis, S.J., Cates, N.L., Bleeker, W., 2017. Sluggish Hadean geodynamics: Evidence from coupled ^{146,147}Sm-^{142,143}Nd systematics in Eoarchean supracrustal rocks of the Inukjuak domain (Québec). Earth Planet. Sci. Lett. 457, 23–37.

Cawthorn, R.G., 1975. Degrees of melting in mantle diapirs and the origin of ultrabasic liquids. Earth Planet. Sci. Lett. 27 (1), 113–120.

Chase, C.G., Patchett, P.J., 1988. Stored mafic/ultramafic crust and early Archaean mantle differentiation. Earth Planet. Sci. Lett. 91 (1-2), 66–72.

Chou, C.-L., 1978. Fractionation of siderophile elements in the earth's upper mantle. In: Proceedings of the 9th Lunar and Planetary Science Conference, pp. 219–230.

Chou, C.-L., Shaw, D.M., Crocket, J.H., 1983. Siderophile trace elements in the Earth's oceanic crust and upper mantle. J. Geophys. Res. 88 (S2), A507–A518.

Coltice, N., Schmalzl, J., 2006. Mixing times in the mantle of the early Earth derived from 2-D and 3-D numerical simulations of convection. Geophys. Res. Lett. 33 (23), L23304.

Condie, K.C., 1975. Mantle-plume model for the origin of Archaean greenstone belts based on trace element distributions. Nature 258 (5534), 413–414.

Condie, K.C., 1981. Archaean greenstone belts. Elsevier, Amsterdam, p. 434.

Condie, K.C., 1994. Greenstones through time. In: Condie, K.C. (Ed.), Archean Crustal Evolution. Elsevier, Amsterdam, pp. 85–120.

Condie, K.C., 2005. High field strength element ratios in Archean basalts: a window to evolving sources of mantle plumes? Lithos 79 (3-4), 491–504.

Cooper, L.B., Ruscitto, D.M., Plank, T., Wallace, P.J., Syracuse, E.M., Manning, C.E., 2012. Global variations in H_2O/Ce: 1. Slab surface temperatures beneath volcanic arcs. Geochem. Geophys. Geosyst. 13 (3), Q03024.

Corgne, A., Wood, B.J., 2002. $CaSiO_3$ and $CaTiO_3$ perovskite-melt partitioning of trace elements: Implications for gross mantle differentiation. Geophys. Res. Lett. 29 (19), 39.1–39.4.

Corgne, A., Wood, B.J., 2004. Trace element partitioning between majoritic garnet and silicate melt at 25 GPa. Phys. Earth Planet. Inter. 143, 407–419.

Corgne, A., Liebske, C., Wood, B.J., Rubie, D.C., Frost, D.J., 2005. Silicate perovskite-melt partitioning of trace elements and geochemical signature of a deep perovskitic reservoir. Geochim. Cosmochim. Acta 69 (2), 485–496.

Cottrell, E., Walker, D., 2006. Constraints on core formation from Pt partitioning in mafic silicate liquids at high temperatures. Geochim. Cosmochim. Acta 70 (6), 1565–1580.

Courtillot, V., Davaille, A., Besse, J., Stock, J., 2003. Three distinct types of hotspots in the Earth's mantle. Earth Planet. Sci. Lett. 205 (3), 295–308.

Crocket, J.H., Fleet, M.E., Stone, W.E., 1997. Implications of composition for experimental partitioning of platinum-group elements and gold between sulfide liquid and basalt melt: The significance of nickel content. Geochim. Cosmochim. Acta 61 (19), 4139–4149.

Dale, C.W., Kruijer, T.S., Burton, K.W., 2017. Highly siderophile element and ^{182}W evidence for a partial late veneer in the source of 3.8 Ga rocks from Isua, Greenland. Earth and Planetary Science Letters 458, 394–404.

Dauphas, N., Burkhardt, C., Warren, P.H., Fang-Zhen, T., 2014. Geochemical arguments for an Earth-like Moon-forming impactor. Philos. Trans. R. Soc. 372 (2024), 20130244.

Day, J.M.D., 2013. Hotspot volcanism and highly siderophile elements. Chem. Geol. 341, 50–74.

Day, J.M.D., Walker, R.J., 2015. Highly siderophile element depletion in the Moon. Earth Planet. Sci. Lett. 423, 114–124.

Day, J.M.D., Pearson, D.G., Taylor, L.A., 2007. Highly siderophile element constraints on accretion and differentiation of the Earth-Moon system. Science 315 (5809), 217–219.

Day, J.M.D., Walker, R.J., James, O.B., Puchtel, I.S., 2010. Osmium isotope and highly siderophile element systematics of the lunar crust. Earth Planet. Sci. Lett. 289 (3-4), 595–605.

Day, J.M.D., Brandon, A.D., Walker, R.J., 2016. Highly Siderophile Elements in Earth, Mars, the Moon, and Asteroids. Rev. Mineral. Geochem. 81 (1), 161–238.

De Wit, M.J., Ashwal, L.D., 1997. Greenstone Belts. Clarendon Press, Oxford, p. 809.

Debaille, V., O'Neill, C., Brandon, A.D., Haenecour, P., Yin, Q.-Z., Mattielli, N., Treiman, A.H., 2013. Stagnant-lid tectonics in early Earth revealed by ^{142}Nd variations in late Archean rocks. Earth Planet. Sci. Lett. 373, 83–92.

DePaolo, D.J., 1980. Crustal growth and mantle evolution: inferences from models of element transport and Nd and Sr isotopes. Geochim. Cosmochim. Acta 44 (8), 1185–1196.

DePaolo, D.J., Wasserburg, G.J., 1976. Nd isotopic variations and petrogenetic models. Geophys. Res. Lett. 3 (5), 249–252.

Desrochers, J.-P., Hubert, C., Ludden, J.N., Pilote, P., 1993. Accretion of Archaean oceanic plateau fragments in the Abitibi greenstone belt, Canada. Geology 21 (5), 451–454.

Dostal, J., Mueller, W.U., 2013. Deciphering an Archean mantle plume: Abitibi greenstone belt, Canada. Gondwana Res. 23 (2), 493–505.

Drake, M.J., 2000. Accretion and primary differentiation of the Earth: A personal journey. Geochim. Cosmochim. Acta 64 (14), 2363–2370.

Dupré, B., Chauvel, C., Arndt, N.T., 1984. Pb and Nd isotopic study of two Archean komatiitic flows from Alexo, Ontario. Geochim. Cosmochim. Acta 48 (10), 1965–1972.

Dziewonski, A.M., Hager, B.H., O'Connell, R.J., 1977. Large-scale heterogeneities in the lower mantle. J. Geophys. Res. 82 (2), 239–255.

Elkins-Tanton, L.T., 2008. Linked magma ocean solidification and atmospheric growth for Earth and Mars. Earth Planet. Sci. Lett. 271 (1-4), 181–191.

Elkins-Tanton, L.T., 2012. Magma Oceans in the Inner Solar System. Annu. Rev. Earth Planet. Sci. 40 (1), 113–139.

Farnetani, C.G., 1997. Excess temperature of mantle plumes: the role of chemical stratification across "D". Geophys. Res. Lett. 24 (13), 1583–1586.

Farnetani, C.G., Richards, M.A., 1995. Thermal entrainment and melting in mantle plumes. Earth Planet. Sci. Lett. 136 (4), 251–267.

Fischer-Gödde, M., Becker, H., Wombacher, F., 2010. Rhodium, gold and other highly siderophile element abundances in chondritic meteorites. Geochim. Cosmochim. Acta 74 (1), 356–379.

Fischer-Gödde, M., Becker, H., Wombacher, F., 2011. Rhodium, gold and other highly siderophile elements in orogenic peridotites and peridotite xenoliths. Chem. Geol. 280 (3-4), 365–383.

Fletcher, M., Wyman, D.A., 2015. Mantle plume-subduction zone interactions over the past 60 Ma. Lithos 233, 162–173.

Foley, B.J., Rizo, H., 2017. Long-term preservation of early formed mantle heterogeneity by mobile lid convection: Importance of grainsize evolution. Earth Planet. Sci. Lett. 475, 94–105.

Foley, S.F., Barth, M.G., Jenner, G.A., 2000. Rutile/melt partition coefficients for trace elements and an assessment of the influence of rutile on the trace element characteristics of subduction zone magmas. Geochim. Cosmochim. Acta 64 (5), 933–938.

Fortenfant, S.S., Gunther, D., Dingwell, D.B., Rubie, D.C., 2003. Temperature dependence of Pt and Rh solubilities in a haplobasaltic melt. Geochim. Cosmochim. Acta 67 (1), 123–131.

French, S.W., Romanowicz, B., 2015. Broad plumes rooted at the base of the Earth's mantle beneath major hotspots. Nature 525 (7567), 95–99.

Frost, D.J., Mann, U., Asahara, Y., Rubie, D.C., 2008. The redox state of the mantle during and just after core formation. Philos. Trans. R. Soc. 366 (1883), 4315–4337.

Galer, S.J.G., Goldstein, S.L., 1991. Early mantle differentiation and its thermal consequences. Geochim. Cosmochim. Acta 55 (1–2), 227–239.

Galer, S.J.G., Goldstein, S.L., O'Nions, R.K., 1989. Limits on chemical and convective isolation in the Earth's interior. Chem. Geol. 75 (4), 257–290.

Gerya, T., 2014. Precambrian geodynamics: Concepts and models. Gondwana Res. 25 (2), 442–463.

Goldstein, S.L., Galer, S.J.G., 1992. On the trail of early mantle differentiation: ^{142}Nd/^{144}Nd ratios of early Archean rocks. Eos 73 (30), 323.

Goldstein, S.L., O'Nions, R.K., Hamilton, P.J., 1984. A Sm-Nd isotopic study of atmospheric dusts and particulates from major river systems. Earth Planet. Sci. Lett. 70 (2), 221–236.

Green, D.H., 1975. Genesis of Archean peridotitic magmas and constraints on Archean geothermal gradients and tectonics. Geology 3 (1), 15–18.

Green, D.H., 1981. Petrogenesis of Archean ultramafic magmas and implications for Archean tectonics. In: Kröner, A. (Ed.), Precambrian Plate Tectonics. Elsevier, Amsterdam, pp. 469–480.

Grove, T.L., Parman, S.W., 2004. Thermal evolution of the Earth as recorded by komatiites. Earth Planet. Sci. Lett. 219 (3-4), 173–187.

Griffiths, R.W., Campbell, I.H., 1990. Stirring and structure in mantle starting plumes. Earth Planet. Sci. Lett. 99 (1–2), 66–78.

Grove, T.L., de Wit, M.J., Dann, J., 1997. Komatiites from the Komati type section, Barberton, South Africa. In: de Wit, M.J., Ashwal, L.D. (Eds.), Greenstone Belts. Oxford Science Publications, Oxford, pp. 422–437.

Hamilton, P.J., O'Nions, R.K., Bridgwater, D., Nutman, A.P., 1983. Sm-Nd studies of Archaean metasediments and metavolcanics from West Greenland and their implications for the Earth's early history. Earth Planet. Sci. Lett. 62 (2), 263–272.

Harper, C.L., Jacobsen, S.B., 1992. Evidence from coupled ^{147}Sm-^{143}Nd and ^{146}Sm-^{142}Nd systematics for very early (4.5-Gyr) differentiation of the Earth's mantle. Nature 360 (6406), 728–732.

Harper, C.L., Jacobsen, S.B., 1996. Evidence for ^{182}Hf in the early Solar System and constraints on the timescale of terrestrial accretion and core formation. Geochim. Cosmochim. Acta 60 (7), 1131–1153.

Hart, S.R., Brooks, S., 1977. The geochemistry and evolution of Early Precambrian mantle. Contrib. Mineral. Petrol. 61 (2), 109–128.

Hart, S.R., Zindler, A., 1986. In search of a bulk-earth composition. Chem. Geol. 57 (3–4), 247–267.

Hart, S.R., Hauri, E.H., Oschmann, L.A., Whitehead, J.A., 1992. Mantle plumes and entrainment: isotopic evidence. Science 256 (5056), 517–520.

Hauri, E.H., Gaetani, G.A., Green, T.H., 2006. Partitioning of water during melting of the Earth's upper mantle at H_2O-undersaturated conditions, 248 (3-4), 715–734.

He, Y., Wen, L., Capdeville, Y., Zhao, L., 2015. Seismic evidence for an Iceland thermo-chemical plume in the Earth's lowermost mantle. Earth Planet. Sci. Lett. 417, 19–27.

Herzberg, C.T., 1992. Depth and degree of melting of komatiites. J. Geophys. Res. 97 (B4), 4521–4540.

Herzberg, C.T., 1995. Generation of plume magmas through time: an experimental perspective. Chem. Geol. 126 (1), 1–16.

Herzberg, C., Gazel, E., 2009. Petrological evidence for secular cooling in mantle plumes. Nature 458 (7238), 619–622.

Herzberg, C., O'Hara, M.J., 2002. Plume-associated ultramafic magmas of Phanerozoic age. J. Petrol. 43 (10), 1857–1883.

Herzberg, C.T., Ohtani, E., 1988. Origin of komatiite at high pressures. Earth Planet. Sci. Lett. 88 (3-4), 321–329.

Herzberg, C., Asimow, P.D., 2008. Petrology of some oceanic island basalts: PRIMELT2. XLS software for primary magma calculation. Geochem. Geophys. Geosyst. 9 (9), Q09001.

Herzberg, C., Asimow, P.D., Arndt, N.T., Niu, Y.L., Lesher, C.M., Fitton, J.G., Cheadle, M. J., Saunders, A.D., 2007. Temperatures in ambient mantle and plumes: Constraints from basalts, picrites, and komatiites. Geochem. Geophys. Geosyst. 8, Q02006.

Herzberg, C., Condie, K., Korenaga, J., 2010. Thermal history of the Earth and its petrological expression. Earth Planet. Sci. Lett. 292 (1-2), 79–88.

Hickman, A., Kranendonk, M.V., 2012. Early Earth Evolution: Evidence from the 3.5-1.8 Ga Geological History of the Pilbara Region of Western Australia. Episodes 35 (1), 283–297.

Hirschmann, M.M., 2018. Comparative deep Earth volatile cycles: The case for C recycling from exosphere/mantle fractionation of major (H_2O, C, N) volatiles and from H_2O/Ce, CO_2/Ba, and CO_2/Nb exosphere ratios. Earth Planet. Sci. Lett. 502, 262–273.

Hoffmann, J.E., Wilson, A.H., 2017. The origin of highly radiogenic Hf isotope compositions in 3.33 Ga Commondale komatiite lavas (South Africa). Chem. Geol. 455, 6–21.

Hoffmann, J.E., Münker, C., Polat, A., Rosing, M.T., Schulz, T., 2011. The origin of decoupled Hf-Nd isotope compositions in Eoarchean rocks from southern West Greenland. Geochim. Cosmochim. Acta 75 (21), 6610–6628.

Hofmann, A.W., 1988. Chemical differentiation of the Earth: The relationship between mantle, continental crust and oceanic crust. Earth Planet. Sci. Lett. 90 (3), 297–314.

Hofmann, A.W., Hart, S., 1978. An assessment of local and regional isotopic equilibrium in the mantle. Earth Planet. Sci. Lett. 38 (1), 44–62.

Hofmann, A.W., White, W.M., 1982. Mantle plumes from ancient oceanic crust. Earth Planet. Sci. Lett. 57 (2), 421–436.

Hofmann, A.W., Jochum, K.P., Seufert, M., White, W.M., 1986. Nb and Pb in oceanic basalts: New constraints on mantle evolution. Earth Planet. Sci. Lett. 79 (1-2), 33–45.

Horan, M.F., Walker, R.J., Morgan, J.W., Grossman, J.N., Rubin, A.E., 2003. Highly siderophile elements in chondrites. Chem. Geol. 196 (1-4), 5–20.

Horan, M.F., Carlson, R.W., Walker, R.J., Jackson, M., Garçon, M., Norman, M., 2018. Tracking Hadean processes in modern basalts with 142-Neodymium. Earth Planet. Sci. Lett. 484, 184–191.

Humayun, M., 2011. A model for osmium isotopic evolution of metallic solids at the core-mantle boundary. Geochem. Geophys. Geosyst. 12 (3), 1–23.

Huppert, H.E., Sparks, R.S.J., 1985. Cooling and contamination of mafic and ultramafic magmas during ascent through continental crust. Earth Planet. Sci. Lett. 74 (4), 371–386.

Huppert, H.E., Sparks, R.S.J., Turner, J.S., Arndt, N.T., 1984. Emplacement and cooling of komatiite lavas. Nature 309 (5963), 19–22.

Hyung, E., Jacobsen, S.B., 2020. The ^{142}Nd/^{144}Nd variations in mantle-derived rocks provide constraints on the stirring rate of the mantle from the Hadean to the present. Proc. Natl. Acad. Sci. 117 (26), 14738–14744.

Ireland, T.J., Walker, R.J., Garcia, M.O., 2009. Highly siderophile element and 187Os isotope systematics of Hawaiian picrites: Implications for parental melt composition and source heterogeneity. Chem. Geol. 260 (1-2), 112–128.

Ito, E., Kubo, A., Katsura, T., Walter, M.J., 2004. Melting experiments of mantle materials under lower mantle conditions with implications for magma ocean differentiation. Phys. Earth Planet. Inter. 143, 397–406.

Jackson, M.G., Carlson, R.W., 2012. Homogeneous superchondritic ^{142}Nd/^{144}Nd in the mid-ocean ridge basalt and ocean island basalt mantle. Geochem. Geophys. Geosyst. 13 (6), Q06011.

Jacobsen, S.B., 1988. Isotopic and chemical constraints on mantle-crust evolution. Geochim. Cosmochim. Acta 52 (6), 1341–1350.

Jacobsen, S.B., Wasserburg, G.J., 1979. Mean Age of mantle and crustal reservoirs. J. Geophys. Res. 84 (NB13), 7411–7427.

Jacobsen, S.B., Wasserburg, G.J., 1980. Sm-Nd isotopic evolution of chondrites. Earth Planet. Sci. Lett. 50 (1), 139–155.

Jacobsen, S.B., Yu, G., 2015. Extinct isotope heterogeneities in the mantles of Earth and Mars: Implications for mantle stirring rates. Meteorit. Planet. Sci. 50 (4), 555–567.

Jahn, B.-M., Gruau, G., Glikson, A.Y., 1982. Komatiites of the Onverwacht Group, South Africa: REE geochemistry, Sm-Nd age and mantle evolution. Contrib. Mineral. Petrol. 80 (1), 25–40.

Jamais, M., Lassiter, J.C., Brügmann, G., 2008. PGE and Os-isotopic variations in lavas from Kohala Volcano, Hawaii: Constraints on PGE behavior and melt/crust interaction. Chem. Geol. 250 (1-4), 16–28.

Jenner, F.E., O'Neill, H., St.C.C.Q., 2012. Major and trace analysis of basaltic glasses by laser-ablation ICP-MS. Geochem. Geophys. Geosyst. 13 (3), Q03003.

Jochum, K.P., Arndt, N.T., Hofmann, A.W., 1991. Nb-Th-La in komatiites and basalts: constraints on komatiite petrogenesis and mantle evolution. Earth Planet. Sci. Lett. 107 (2), 272–289.

Johnson, T.E., Brown, M., Gardiner, N.J., Kirkland, C.L., Smithies, R.H., 2017. Earth's first stable continents did not form by subduction. Nature 543 (7644), 239–242.

Kato, T., Ringwood, A.E., Irifune, T., 1988. Experimental determination of element partitioning between silicate perovskite, garnet and liquid: constraints on early differentiation of the mantle. Earth Planet. Sci. Lett. 89 (1), 123–145.

Kent, R.W., Hardarson, B.S., Saunders, A.D., Storey, M., 1996. Plateaux ancient and modern: Geochemical and sedimentological perspectives on Archaean oceanic magmatism. Lithos 37 (2-3), 129–142.

Kimura, K., Lewis, R.S., Anders, S., 1974. Distribution of gold and rhenium between nickel-iron and silicate melts; implications for abundance of siderophile elements on the Earth and Moon. Geochim. Cosmochim. Acta 38 (5), 683–701.

Kimura, G., Ludden, J.N., Desroshers, J.-P., Hori, R., 1993. A model of ocean-crust accretion for the Superior province, Canada. Lithos 30 (3-4), 337–355.

Kleine, T., Walker, R.J., 2017. Tungsten Isotopes in Planets. Annu. Rev. Earth Planet. Sci. 45 (1), 389–417.

Kleine, T., Münker, C., Mezger, K., Palme, H., 2002. Rapid accretion and early core formation on asteroids and the terrestrial planets from Hf-W chronometry. Nature 418 (6901), 952–955.

Kleine, T., Mezger, K., Palme, H., Münker, C., 2004. The W isotope evolution of the bulk silicate Earth: constraints on the timing and mechanisms of core formation and accretion. Earth Planet. Sci. Lett. 228 (1-2), 109–123.

Kleine, T., Touboul, M., Bourdon, B., Nimmo, F., Mezger, K., Palme, H., Jacobsen, S.B., Yin, Q.-Z., Halliday, A.N., 2009. Hf-W chronology of the accretion and early evolution of asteroids and terrestrial planets. Geochim. Cosmochim. Acta 73 (17), 5150–5188.

König, S., Münker, C., Schuth, S., Garbe-Schönberg, D., 2008. Mobility of tungsten in subduction zones. Earth Planet. Sci. Lett. 274 (1-2), 89–92.

König, S., Münker, C., Hohl, S., Paulick, H., Barth, A.R., Lagos, M., Pfander, J., Büchl, A., 2011. The Earth's tungsten budget during mantle melting and crust formation. Geochim. Cosmochim. Acta 75 (8), 2119–2136.

Koppers, A.A.P., Becker, T.W., Jackson, M.G., Konrad, K., Müller, R.D., Romanowicz, B., Steinberger, B., Whittaker, J.M., 2021. Mantle plumes and their role in Earth processes. Nat. Rev. 2, 382–401.

Korenaga, J., 2021. Hadean geodynamics and the nature of early continental crust. Precambrian Res. 359, 106178.

Kruijer, T.S., Kleine, T., 2017. Tungsten isotopes and the origin of the Moon. Earth Planet. Sci. Lett. 475 (Supplement C), 15–24.

Kruijer, T.S., Kleine, T., Fischer-Gödde, M., Sprung, P., 2015. Lunar tungsten isotopic evidence for the late veneer. Nature 520 (7548), 534–537.

Kusky, T.M., Kidd, W.S.F., 1992. Remnants of an Archean oceanic plateau, Belingwe greenstone belt, Zimbabwe. Geology 20 (1), 43–46.

Labrosse, S., Hernlund, J.W., Coltice, N., 2007. A crystallizing dense magma ocean at the base of the Earth's mantle. Nature 450 (7171), 866–869.

Lassiter, J.C., 2006. Constraints on the coupled thermal evolution of the Earth's core and mantle, the age of the inner core, and the origin of the ^{186}Os/^{188}Os "core signal" in plume-derived lavas. Earth Planet. Sci. Lett. 250 (1-2), 306–317.

Lassiter, J.C., Hauri, E.H., 1998. Osmium-isotope variations in Hawaiian lavas: evidence for recycled oceanic lithosphere in the Hawaiian plume. Earth Planet. Sci. Lett. 164 (3-4), 483–496.

Liebske, C., Corgne, A., Frost, D.J., Rubie, D.C., Wood, B.J., 2005. Compositional effects on element partitioning between Mg-silicate perovskite and silicate melts. Contrib. Mineral. Petrol. 149 (1), 113–128.

Liu, J., Touboul, M., Ishikawa, A., Walker, R.J., Pearson, D.G., 2016. Widespread tungsten isotope anomalies and W mobility in crustal and mantle rocks of the Eoarchean Saglek Block, northern Labrador, Canada: Implications for early Earth processes and W recycling. Earth Planet. Sci. Lett. 448, 13–23.

Loper, D.E., 1991. Mantle plumes. Tectonophysics 187 (4), 373–384.

Maier, W.D., Barnes, S.J., Campbell, I.H., Fiorentini, M.L., Peltonen, P., Barnes, S.-J., Smithies, R.H., 2009. Progressive mixing of meteoritic veneer into the early Earth's deep mantle. Nature 460 (7255), 620–623.

Mallmann, G., O'Neill, H., 2007. The effect of oxygen fugacity on the partitioning of Re between crystals and silicate melt during mantle melting. Geochim. Cosmochim. Acta 71 (11), 2837–2857.

Marchi, S., Canup, R.M., Walker, R.J., 2018. Heterogeneous delivery of silicate and metal to the Earth by large planetesimals. Nat. Geosci. 11, 77–81.

Marchi, S., Walker, R.J., Canup, R.M., 2020. A compositionally heterogeneous martian mantle due to late accretion. Science. Advances 6 (7), eaay2338.

Maya, J.M., Bhutani, R., Balakrishnan, S., Rajee Sandhya, S., 2017. Petrogenesis of 3.15 Ga old Banasandra komatiites from the Dharwar craton, India: Implications for early mantle heterogeneity. Geosci. Front. 8 (3), 467–481.

McDonough, W.F., Sun, S.S., 1995. The composition of the Earth. Chem. Geol. 120 (3-4), 223–253.

McKenzie, D., Bickle, M.J., 1988. The volume and composition of melt generated by extension of the lithosphere. J. Petrol. 29 (3), 625–679.

Meisel, T., Walker, R.J., Irving, A.J., Lorand, J.-P., 2001. Osmium isotopic compositions of mantle xenoliths: A global perspective. Geochim. Cosmochim. Acta 65 (8), 1311–1323.

Michael, P., 1995. Regionally Distinctive Sources of Depleted MORB - Evidence from Trace-Elements and H_2O. Earth Planet. Sci. Lett. 131 (3-4), 301–320.

Mole, D.R., Fiorentini, M.L., Thebaud, N., Cassidy, K.F., McCuaig, T.C., Kirkland, C.L., Romano, S.S., Doublier, M.P., Belousova, E.A., Barnes, S.J., Miller, J., 2014. Archean komatiite volcanism controlled by the evolution of early continents. Proc. Natl. Acad. Sci. 111 (28), 10083–10088.

Montelli, R., Nolet, G., Dahlen, F.A., Masters, G., Engdahl, E.R., Hung, S.-H., 2004. Finite-Frequency Tomography Reveals a Variety of Plumes in the Mantle. Science 303 (5656), 338–343.

Moore, J.G., 1970. Water Content of Basalt Erupted on the ocean floor. Contrib. Mineral. Petrol. 28 (4), 272–279.

Morino, P., Caro, G., Reisberg, L., Schumacher, A., 2017. Chemical stratification in the post-magma ocean Earth inferred from coupled ^{146,147}Sm-^{142,143}Nd systematics in ultramafic rocks of the Saglek block (3.25-3.9 Ga; northern Labrador, Canada). Earth Planet. Sci. Lett. 463, 136–150.

Mundl, A., Touboul, M., Jackson, M.G., Day, J.M.D., Kurz, M.D., Lekic, V., Helz, R.T., Walker, R.J., 2017. Tungsten-182 heterogeneity in modern ocean island basalts. Science 356 (6333), 66–69.

Mundl, A., Walker, R.J., Reimink, J.R., Rudnick, R.L., Gaschnig, R.M., 2018. Tungsten-182 in the upper continental crust: Evidence from glacial diamictites. Chem. Geol. 494, 144–152.

Mundl-Petermeier, A., Walker, R.J., Jackson, M.G., Blichert-Toft, J., Kurz, M.D., Haldórsson, S.A., 2019. Temporal evolution of primordial tungsten-182 and ^{3}He/^{4}He signatures in the Iceland mantle plume. Chem. Geol. 525, 245–259.

Mundl-Petermeier, A., Walker, R.J., Fischer, R.A., Lekic, V., Jackson, M.G., Kurz, M.D., 2020. Anomalous μ^{182}W signatures in high ^{3}He/^{4}He ocean island basalts – fingerprints of Earth's core? Geochim. Cosmochim. Acta 271, 194–211.

Murphy, D.T., Brandon, A.D., Debaille, V., Burgess, R., Ballentine, C., 2010. In search of a hidden long-term isolated sub-chondritic ^{142}Nd/^{144}Nd reservoir in the deep mantle: Implications for the Nd isotope systematics of the Earth. Geochim. Cosmochim. Acta 74 (2), 738–750.

Murphy, D., Rizo, H., O'Neil, J., Hepple, R., Wiemer, D., Kemp, A., Vervoort, J., 2021. Combined Sm-Nd, Lu-Hf, and ^{142}Nd study of Paleoarchean basalts from the East Pilbara Terrane, Western Australia. Chemical Geology 578, 120301.

Nakagawa, T., 2020. A coupled core-mantle evolution: review and future prospects. Progr. Earth Planet. Sci. 7 (1), 57.

Nakanishi, N., Giuliani, A., Carlson, R.W., Horan, M.F., Woodhead, J., Pearson, D.G., Walker, R.J., 2021. Tungsten-182 evidence for an ancient kimberlite source. Proc. Natl. Acad. Sci. 118 (23), e2020680118.

Nesbitt, R.W., Sun, S.S., Purvis, A.C., 1979. Komatiites: geochemistry and genesis. Can. Mineral. 17 (2), 165–186.

Newsom, H.E., Sims, K.W.W., Noll, P.D., Jaeger, W.L., Maehr, S.A., Beserra, T.B., 1996. The depletion of tungsten in the bulk silicate Earth: Constraints on core formation. Geochim. Cosmochim. Acta 60 (5), 1155–1169.

Nicklas, R.W., Puchtel, I.S., Ash, R.D., 2018. The Redox Evolution of the Archean Mantle: Evidence from Komatiites. Geochim. Cosmochim. Acta 222, 447–466.

Nicklas, R.W., Puchtel, I.S., Ash, R.D., Piccoli, P.M., Hanski, E., Nisbet, E.G., Waterton, P., Pearson, D.G., Anbar, A.D., 2019. Secular mantle oxidation across the Archean-Proterozoic boundary: Evidence from V partitioning in komatiites and picrites. Geochim. Cosmochim. Acta 250, 49–75.

Nisbet, E.G., Cheadle, M.J., Arndt, N.T., Bickle, M.J., 1993. Constraining the potential temperature of the Archaean mantle: a review of the evidence from komatiites. Lithos 30, 291–307.

O'Neill, C., Debaille, V., 2014. The evolution of Hadean-Eoarchaean geodynamics. Earth Planet. Sci. Lett. 406, 49–58.

Ohtani, E., 1984. Generation of komatiite magma and gravitational differentiation in the deep upper mantle. Earth Planet. Sci. Lett. 67 (2), 261–272.

O'Neil, J., Carlson, R.W., Francis, D., Stevenson, R.K., 2008. Neodymium-142 evidence for Hadean mafic crust. Science 321 (5897), 1828–1831.

O'Neil, J., Carlson, R.W., Paquette, J.-L., Francis, D., 2012. Formation age and metamorphic history of the Nuvvuagittuq Greenstone Belt. Precambrian Res. 220-221, 23–44.

O'Neil, J., Rizo, H., Boyet, M., Carlson, R.W., Rosing, M.T., 2016. Geochemistry and Nd isotopic characteristics of Earth's Hadean mantle and primitive crust. Earth Planet. Sci. Lett. 442, 194–205.

Parman, S.W., Dann, J.C., Grove, T.L., de Wit, M.J., 1997. Emplacement conditions of komatiite magmas from the 3.49 Ga Komati Formation, Barberton greenstone belt, South Africa. Earth Planet. Sci. Lett. 150 (3-4), 303–323.

Parman, S.W., Grove, T.L., Dann, J.C., 2001. The production of Barberton komatiites in an Archean subduction zone. Geophys. Res. Lett. 28 (13), 2513–2516.

Parman, S.W., Grove, T.L., Dann, J.C., de Wit, M.J., 2004. S. Afr. J. Geol. 107 (1-2), 107–118.

Patchett, P.J., Tatsumoto, M., 1980. Hafnium isotope variations in oceanic basalts. Geophys. Res. Lett. 7 (12), 1077–1080.

Patchett, P.J., Kauvo, O., Hedge, C.E., Tatsumoto, M., 1981. Evolution of continental crust and mantle heterogeneity: evidence from Hf isotopes. Contrib. Mineral. Petrol. 78 (3), 279–297.

Patchett, P.J., White, W.M., Feldmann, H., Kielinczuk, S., Hofmann, A.W., 1984. Hafnium/rare earth element fractionation in the sedimentary system and crustal recycling into the Earth's mantle. Earth Planet. Sci. Lett. 69 (2), 365–378.

Peters, B.J., Carlson, R.W., Day, J.M.D., Horan, M.F., 2018. Hadean silicate differentiation preserved by anomalous ^{142}Nd/^{144}Nd ratios in the Réunion hotspot source. Nature 555, 89–106.

Peters, B.J., Mundl-Petermeier, A., Carlson, R.W., Walker, R.J., Day, J.M.D., 2021. Combined lithophile-siderophile isotopic constraints on Hadean processes preserved in ocean island basalt sources. Geochem. Geophys. Geosyst. 22 (3) e2020GC009479.

Puchtel, I.S., Humayun, M., 2000. Platinum group elements in Kostomuksha komatiites and basalts: Implications for oceanic crust recycling and core-mantle interaction. Geochim. Cosmochim. Acta 64 (24), 4227–4242.

Puchtel, I.S., Humayun, M., 2005. Highly siderophile element geochemistry of ^{187}Os-enriched 2.8-Ga Kostomuksha komatiites, Baltic Shield. Geochim. Cosmochim. Acta 69 (6), 1607–1618.

Puchtel, I.S., Brügmann, G.E., Hofmann, A.W., 2001. 187Os-enriched domain in an Archaean mantle plume: evidence from 2.8 Ga komatiites of the Kostomuksha greenstone belt, NW Baltic Shield. Earth Planet. Sci. Lett. 186 (3–4), 513–526.

Puchtel, I.S., Hofmann, A.W., Mezger, K., Jochum, K.P., Shchipansky, A.A., Samsonov, A. V., 1998. Oceanic plateau model for continental crustal growth in the Archaean: A case study from the Kostomuksha greenstone belt, NW Baltic Shield. Earth Planet. Sci. Lett. 155 (1-2), 57–74.

Puchtel, I.S., Brandon, A.D., Humayun, M., 2004a. Precise Pt-Re-Os isotope systematics of the mantle from 2.7-Ga komatiites. Earth Planet. Sci. Lett. 224 (1-2), 157–174.

Puchtel, I.S., Humayun, M., Campbell, A., Sproule, R., Lesher, C.M., 2004b. Platinum group element geochemistry of komatiites from the Alexo and Pyke Hill areas, Ontario, Canada. Geochimica et Cosmochimica Acta 68 (6), 1361–1383.

Puchtel, I.S., Brandon, A.D., Humayun, M., Walker, R.J., 2005. Evidence for the early differentiation of the core from Pt-Re-Os isotope systematics of 2.8-Ga komatiites. Earth Planet. Sci. Lett. 237 (1-2), 118–134.

Puchtel, I.S., Humayun, M., Walker, R.J., 2007. Os-Pb-Nd isotope and highly siderophile and lithophile trace element systematics of komatiitic rocks from the Volotsk suite, SE Baltic Shield. Precambrian Res. 158 (1-2), 119–137.

Puchtel, I.S., Walker, R.J., Brandon, A.D., Nisbet, E.G., 2009a. Pt-Re-Os and Sm-Nd isotope and HSE and REE systematics of the 2.7 Ga Belingwe and Abitibi komatiites. Geochim. Cosmochim. Acta 73 (20), 6367–6389.

Puchtel, I.S., Walker, R.J., Anhaeusser, C.R., Gruau, G., 2009b. Re-Os isotope systematics and HSE abundances of the 3.5 Ga Schapenburg komatiites, South Africa: Hydrous melting or prolonged survival of primordial heterogeneities in the mantle? Chem. Geol. 262 (3–4), 355–369.

Puchtel, I.S., Blichert-Toft, J., Touboul, M., Walker, R.J., Byerly, G., Nisbet, E.G., Anhaeusser, C.R., 2013. Insights into early Earth from Barberton komatiites: Evidence from lithophile isotope and trace element systematics. Geochim. Cosmochim. Acta 108, 63–90.

Puchtel, I.S., Walker, R.J., Touboul, M., Nisbet, E.G., Byerly, G.R., 2014. Insights into early Earth from the Pt-Re-Os isotope and highly siderophile element abundance systematics of Barberton komatiites. Geochim. Cosmochim. Acta 125, 394–413.

Puchtel, I.S., Blichert-Toft, J., Touboul, M., Horan, M.F., Walker, R.J., 2016a. The coupled ^{182}W-^{142}Nd record of early terrestrial mantle differentiation. Geochem. Geophys. Geosyst. 17 (6), 2168–2193.

Puchtel, I.S., Touboul, M., Blichert-Toft, J., Walker, R.J., Brandon, A.D., Nicklas, R.W., Kulikov, V.S., Samsonov, A.V., 2016b. Lithophile and siderophile element systematics of the mantle at the Archean-Proterozoic boundary: Evidence from 2.4 Ga komatiites. Geochim. Cosmochim. Acta 180, 227–255.

Puchtel, I.S., Blichert-Toft, J., Touboul, M., Walker, R.J., 2018. ^{182}W and HSE constraints from 2.7 Ga komatiites on the heterogeneous nature of the Archean mantle. Geochim. Cosmochim. Acta 228, 1–26.

Puchtel, I.S., Mundl-Petermeier, A., Horan, M., Hanski, E.J., Blichert-Toft, J., Walker, R. J., 2020. Ultra-depleted 2.05 Ga komatiites of Finnish Lapland: Products of grainy late accretion or core-mantle interaction? Chem. Geol. 554, 119801.

Puchtel, I.S., Nicklas, R.W., Slagle, J., Horan, M., Walker, R.J., Nisbet, E.G., Locmelis, M., 2022. Early global mantle chemical and isotope heterogeneity revealed by the komatiite-basalt record: The Western Australia connection. Geochim. Cosmochim. Acta 320, 238–278.

Rehkämper, M., Halliday, A.N., Fitton, J.G., Lee, D.-C., Wieneke, M., Arndt, N.T., 1999. Ir, Ru, Pt and Pd in basalts and komatiites: New constraints for the geochemical behavior of the platinum group elements in the mantle. Geochim. Cosmochim. Acta 63 (22), 3915–3934.

Reimink, J.R., Chacko, T., Carlson, R.W., Shirey, S.B., Liu, J., Stern, R.A., Bauer, A.M., Pearson, D.G., Heaman, L.M., 2018. Petrogenesis and tectonics of the Acasta Gneiss Complex derived from integrated petrology and ^{142}Nd and ^{182}W extinct nuclide-geochemistry. Earth Planet. Sci. Lett. 494, 12–22.

Reimink, J.R., Mundl-Petermeier, A., Carlson, R.W., Shirey, S.B., Walker, R.J., Pearson, D.G., 2020. Tungsten isotope composition of Archean crustal reservoirs and implications for terrestrial μ^{182}W evolution. Geochem. Geophys. Geosyst. 21 (7) e2020GC009155.

Richard, D., Marty, B., Chaussidon, M., Arndt, N.T., 1996. Helium isotopic evidence for a lower mantle component in depleted Archean komatiite. Science 273 (5271), 93–95.

Richards, M.A., Jones, D.L., Duncan, R.A., DePaolo, D.J., 1991. A mantle plume initiation model for the Wrangellia flood basalt and other oceanic plateaus. Science 254 (5029), 263–265.

Richter, F.M., 1985. Models for the Archean Thermal Regime. Earth Planet. Sci. Lett. 73 (2-4), 350–360.

Richter, F.M., 1988. A major change in the thermal state of the Earth at the Archean-Proterozoic boundary: Consequences for the nature and preservation of continental lithosphere. J. Petrol. Spec. Lithosphere Issue 39-52.

Righter, K., Drake, M.J., 1997. Metal-silicate equilibrium in a homogeneously accreting earth: new results for Re. Earth Planet. Sci. Lett. 146 (3-4), 541–553.

Righter, K., Walker, R.J., Warren, P.H., 2000. Significance of highly siderophile elements and osmium isotopes in the lunar and terrestrial mantles. In: Righter, K., Canup, R. M. (Eds.), Origin of the Earth and Moon. University of Arizona Press, Tucson, AZ, pp. 291–322.

Rizo, H., Boyet, M., Blichert-Toft, J., Rosing, M., 2011. Combined Nd and Hf isotope evidence for deep-seated source of Isua lavas. Earth Planet. Sci. Lett. 312 (3-4), 267–279.

Rizo, H., Boyet, M., Blichert-Toft, J., O'Neil, J., Rosing, M.T., Paquette, J.-L., 2012. The elusive Hadean enriched reservoir revealed by ^{142}Nd deficits in Isua Archaean rocks. Nature 491 (7422), 96–100.

Rizo, H., Boyet, M., Blichert-Toft, J., Rosing, M.T., 2013. Early mantle dynamics inferred from ^{142}Nd variations in Archean rocks from southwest Greenland. Earth Planet. Sci. Lett. 377-378, 324–335.

Rizo, H., Walker, R.J., Carlson, R.W., Touboul, M., Horan, M.F., Puchtel, I.S., Boyet, M., Rosing, M.T., 2016. Early Earth differentiation investigated through ^{142}Nd, ^{182}W, and highly siderophile element abundances in samples from Isua, Greenland. Geochim. Cosmochim. Acta 175, 319–336.

Rizo, H., Andrault, D., Bennett, N.R., Humayun, M., Brandon, A.D., Vlastelic, I., Moine, B., Poirier, A., Bouhifd, M.A., Murphy, D.T., 2019. ^{182}W evidence for core-mantle interaction in the source of mantle plumes. Geochem. Perspect. Letters 11, 6–11.

Rosas, J.C., Korenaga, J., 2018. Rapid crustal growth and efficient crustal recycling in the early Earth: Implications for Hadean and Archean geodynamics. Earth Planet. Sci. Lett. 494, 42–49.

Roth, A.S.G., Bourdon, B., Mojzsis, S.J., Touboul, M., Sprung, P., Guitreau, M., Blichert-Toft, J., 2013. Inherited ^{142}Nd anomalies in Eoarchean protoliths. Earth Planet. Sci. Lett. 361, 50–57.

Roth, A.S.G., Bourdon, B., Mojzsis, S.J., Rudge, J.F., Guitreau, M., Blichert-Toft, J., 2014. Combined ^{147,146}Sm-^{143,142}Nd constraints on the longevity and residence time of early terrestrial crust. Geochem. Geophys. Geosyst. 15 (6), 2329–2345.

Roy-Barman, M., Allègre, C.-J., 1995. ^{187}Os/^{186}Os in oceanic island basalts: tracing oceanic crust recycling in the mantle. Earth Planet. Sci. Lett. 129 (1-4), 145–161.

Rubie, D.C., Frost, D.J., Mann, U., Asahara, Y., Nimmo, F., Tsuno, K., Kegler, P., Holzheid, A., Palme, H., 2011. Heterogeneous accretion, composition and core-mantle differentiation of the Earth. Earth Planet. Sci. Lett. 301 (1-2), 31–42.

Rudnick, R.L., Gao, S., 2014. Composition of the Continental Crust. Treat. Geochem. 1–51.

Rudnick, R.L., Barth, M., Horn, I., McDonough, W.F., 2000. Rutile-bearing refractory eclogites: missing link between continents and depleted mantle. Science 287 (5451), 278–281.

Ryder, G., 2002. Mass flux in the ancient Earth-Moon system and benign implications for the origin of life on Earth. J. Geophys. Res. 107 (E4), 6.1-6.13.

Saal, A.E., Hauri, E.H., Langmuir, C.H., Perfit, M.R., 2002. Vapour undersaturation in primitive mid-ocean-ridge basalt and the volatile content of Earth's upper mantle. Nature 419 (6906), 451–455.

Saji, N.S., Larsen, K., Wielandt, D., Schiller, M., Costa, M.M., Whitehouse, M.J., Rosing, M.T., Bizzarro, M., 2018. Hadean geodynamics inferred from time-varying ^{142}Nd/^{144}Nd in the early Earth rock record. Geochem. Perspect. Letters 7, 43–48.

Salters, V.J.M., White, W.M., 1998. Hf isotope constraints on mantle evolution. Chem. Geol. 145 (3–4), 447–460.

Schneider, K.P., Hoffmann, J.E., Boyet, M., Münker, C., Kröner, A., 2018. Coexistence of enriched and modern-like ^{142}Nd signatures in Archean igneous rocks of the eastern Kaapvaal Craton, southern Africa. Earth Planet. Sci. Lett. 487, 54–66.

Schoenberg, R., Kamber, B.S., Collerson, K.D., Eugster, O., 2002. New W-isotope evidence for rapid terrestrial accretion and very early core formation. Geochim. Cosmochim. Acta 66 (17), 3151–3160.

Schubert, G., Sandwell, D., 1989. Crustal volumes of the continents and of oceanic and continental submarine plateaus. Earth Planet. Sci. Lett. 92 (2), 234–246.

Shirey, S.B., Hanson, G.N., 1986. Mantle heterogeneity and crustal recycling in Archean granite-greenstone belts: Evidence from Nd isotopes and trace elements in the Rainy Lake area, Superior Province, Ontario, Canada. Geochimica et Cosmochimica Acta 50 (12), 2631–2651.

Shirey, S.B., Walker, R.J., 1998. The Re-Os isotope system in cosmochemistry and high-temperature geochemistry. Annu. Rev. Earth Planet. Sci. 26, 423–500.

Shirey, S.B., Kamber, B.S., Whitehouse, M.J., Mueller, P.A., Basu, A.R., 2008. A review of the isotopic and trace element evidence for mantle and crustal processes in the Hadean and Archean: Implications for the onset of plate tectonic subduction. In: Condie, K.C., Pease, V. (Eds.), When Did Plate Tectonics Begin on Planet Earth?, Geological Society of America Special Paper, 440, pp. 1–29.

Sivell, W.J., McCulloch, M.T., 1991. Neodymium isotope evidence for ultra-depleted mantle in the early Proterozoic. Nature 354 (6352), 384–387.

Sizova, E., Gerya, T., Stüwe, K., Brown, M., 2015. Generation of felsic crust in the Archean: A geodynamic modeling perspective. Precambrian Res. 271, 198–224.

Smithies, R.H., Champion, D.C., Van Kranendonk, M.J., Hickman, A.H., 2007. Geochemistry of volcanic rocks of the northern Pilbara Craton, Western Australia. In: Geological Survey of Western Australia, Report 104. Perth, 47 pp.

Sobolev, A.V., Asafov, E.V., Gurenko, A.A., Arndt, N.T., Batanova, V.G., Portnyagin, M. V., Garbe-Schönberg, D., Krasheninnikov, S.P., 2016. Komatiites reveal a hydrous Archaean deep-mantle reservoir. Nature 531 (7596), 628–632.

Sobolev, A.V., Asafov, E.V., Gurenko, A.A., Arndt, N.T., Batanova, V.G., Portnyagin, M. V., Garbe-Schönberg, D., Wilson, A.H., Byerly, G.R., 2019. Deep hydrous mantle reservoir provides evidence for crustal recycling before 3.3 billion years ago. Nature 571 (7766), 555–559.

Sossi, P.A., Eggins, S.M., Nesbitt, R.W., Nebel, O., Hergt, J.M., Campbell, I.H., O'Neill, H., Van Kranendonk, M., Davies, D.R., 2016. Petrogenesis and Geochemistry of Archean Komatiites. J. Petrol. 57 (1), 147–184.

Storey, M., Mahoney, J.J., Kroenke, L.W., Saunders, A.D., 1991. Are oceanic plateaus sites of komatiite formation? Geology 19 (4), 376–379.

Strom, R.G., Malhotra, R., Ito, T., Yoshida, F., Kring, D.A., 2005. The origin of planetary impactors in the inner Solar system. Science 309 (5742), 1847–1850.

Tonks, W.B., Melosh, H.J., 1993. Magma ocean formation due to giant impacts. J. Geophys. Res. 98 (E3), 5319–5333.

Torsvik, T.H., Steinberger, B., Ashwal, L.D., Doubrovine, P.V., Trønnes, R.G., 2016. Earth evolution and dynamics - a tribute to Kevin Burke. Can. J. Earth Sci. 53 (11), 1073–1087.

Touboul, M., Puchtel, I.S., Walker, R.J., 2012. ^{182}W evidence for long-term preservation of early mantle differentiation products. Science 335, 1065–1069.

Touboul, M., Liu, J., O'Neil, J., Puchtel, I.S., Walker, R.J., 2014. New insights into the hadean mantle revealed by ^{182}W and highly siderophile element abundances of supracrustal rocks from the Nuvvuagittuq Greenstone Belt, Quebec, Canada. Chem. Geol. 383, 63–75.

Touboul, M., Puchtel, I.S., Walker, R.J., 2015. Tungsten isotopic evidence for disproportional late accretion to the Earth and Moon. Nature 520 (7548), 530–533.

Trønnes, R.G., Frost, D.J., 2002. Peridotite melting and mineral-melt partitioning of major and minor elements at 22-24.5 GPa. Earth Planet. Sci. Lett. 197 (1-2), 117–131.

Turekian, K.K., Clark, S.P., 1969. Inhomogeneous accumulation of the earth from the primitive solar nebula. Earth Planet. Sci. Lett. 6 (5), 346–348.

Tusch, J., Sprung, P., van de Löcht, J., Hoffmann, J.E., Boyd, A.J., Rosing, M.T., Münker, C., 2019. Uniform ^{182}W isotope compositions in Eoarchean rocks from the Isua region, SW Greenland: The role of early silicate differentiation and missing late veneer. Geochim. Cosmochim. Acta 257, 284–310.

Tusch, J., Münker, C., Hasenstab, E., Jansen, M., Marien, C.S., Kurzweil, F., Van Kranendonk, M.J., Smithies, H., Maier, W., Garbe-Schönberg, D., 2021. Convective isolation of Hadean mantle reservoirs through Archean time. Proc. Natl. Acad. Sci. 118 (2), e2012626118.

Van Kranendonk, M.J., 2008. Two types of Archean continental crust: Plume and plate tectonics on early Earth. Am. J. Sci. 310 (10), 1187–1210.

Vervoort, J.D., Blichert-Toft, J., 1999. Evolution of the depleted mantle: Hf isotope evidence from juvenile rocks through time. Geochim. Cosmochim. Acta 63 (3-4), 533–556.

Vervoort, J.D., Patchett, P.J., Blichert-Toft, J., Albarède, F., 1999. Relationships between Lu-Hf and Sm-Nd isotopic systems in the global sedimentary system. Earth Planet. Sci. Lett. 168 (1-2), 79–99.

Vervoort, J.D., Patchett, P.J., Albarède, F., Blichert-Toft, J., Rudnick, R., Downes, H., 2000. Hf-Nd isotopic evolution of the lower crust. Earth Planet. Sci. Lett. 181 (1-2), 115–129.

Viljoen, M.J., Viljoen, R.P., 1969. The geology and geochemistry of the Lower Ultramafic Unit of the Onverwacht Group and a proposed new class of igneous rocks. Geol. Soc. South Africa Special Publication 2, 55–86.

Wade, J., Wood, B.J., 2005. Core formation and the oxidation state of the Earth. Earth Planet. Sci. Lett. 236 (1-2), 78–95.

Walker, R.J., 2009. Highly siderophile elements in the Earth, Moon and Mars: Update and implications for planetary accretion and differentiation. Chemie der Erde - Geochem. 69 (2), 101–125.

Walker, R.J., 2014. Siderophile element constraints on the origin of the Moon. Philos. Trans. R. Soc. Lond. 372, 20130258.

Walker, R.J., 2016. Siderophile Elements in Tracing Planetary Formation and Evolution. Geochem. Perspect. 5 (1), 1–145.

Walker, R.J., Shirey, S.B., Stecher, O., 1988. Comparative Re-Os, Sm-Nd and Rb-Sr isotope and trace element systematics for Archean komatiite flows from Munro Township, Abitibi belt. Ontario. Earth and Planetary Science Letters 87 (1-2), 1–12.

Walker, R.J., Morgan, J.W., Horan, M.F., 1995. ^{187}Os enrichment in some plumes: evidence for core-mantle interaction? Science 269 (5225), 819–822.

Walker, R.J., Morgan, J.W., Beary, E.S., Smoliar, M.I., Czamanske, G.K., Horan, M.F., 1997. Applications of the ^{190}Pt-^{186}Os isotope system to geochemistry and cosmochemistry. Geochim. Cosmochim. Acta 61 (22), 4799–4807.

Walker, R.J., Horan, M.F., Morgan, J.W., Becker, H., Grossman, J.N., Rubin, A.E., 2002. Comparative ^{187}Re-^{187}Os systematics of chondrites: Implications regarding early solar system processes. Geochim. Cosmochim. Acta 66 (23), 4187–4201.

Walker, R.J., Horan, M.F., Shearer, C.K., Papike, J.J., 2004. Low abundances of highly siderophile elements in the lunar mantle: Evidence for prolonged late accretion. Earth Planet. Sci. Lett. 224 (3-4), 399–413.

Walter, M.J., Nakamura, E., Trønnes, R.G., Frost, D.J., 2004. Experimental constraints on crystallization differentiation in a deep magma ocean. Geochim. Cosmochim. Acta 68 (20), 4267–4284.

White, W.M., Patchett, J., 1984. Hf-Nd-Sr isotopes and incompatible element abundances in island arcs: implications for magma origins and crust-mantle evolution. Earth Planet. Sci. Lett. 67 (2), 167–185.

Widom, E., 1997. Sources of ocean island basalts: A review of the osmium isotope evidence. Physica A: Stat. Mech. Applicat. 244 (1-4), 484–496.

Willbold, M., Elliott, T., Moorbath, S., 2011. The tungsten isotopic composition of the Earth's mantle before the terminal bombardment. Nature 477 (7363), 195–198.

Willbold, M., Mojzsis, S.J., Chen, H.W., Elliott, T., 2015. Tungsten isotope composition of the Acasta Gneiss Complex. Earth Planet. Sci. Lett. 419, 168–177.

Willig, M., Stracke, A., 2019. Earth's chondritic light rare earth element composition: Evidence from the Ce-Nd isotope systematics of chondrites and oceanic basalts. Earth Planet. Sci. Lett. 509, 55–65.

Willig, M., Stracke, A., Beier, C., Salters, V.J.M., 2020. Constraints on mantle evolution from Ce-Nd-Hf isotope systematics. Geochim. Cosmochim. Acta 272, 36–53.

Wilson, A.H., Carlson, R.W., 1989. A Sm-Nd and Pb isotope study of Archaean greenstone belts in the southern Kaapvaal Craton, South Africa. Earth Planet. Sci. Lett. 96 (1-2), 89–105.

Wyman, D.A., 2013. A critical assessment of Neoarchean "plume only" geodynamics: Evidence from the Superior Province. Precambrian Res. 229, 3–19.

Wyman, D., 2019. Do cratons preserve evidence of stagnant lid tectonics? Geosci. Front. 9 (1), 3–17.

Wyman, D., 2020. Komatiites From Mantle Transition Zone Plumes. Front. Earth Sci. 8 (383), 540744.

Yin, Q., Jacobsen, S.B., Yamashita, K., Blichert-Toft, J., Telouk, P., Albarede, F., 2002. A short timescale for terrestrial planet formation from Hf-W chronometry of meteorites. Nature 418 (6901), 949–952.

Yokoyama, T., Walker, D., Walker, R.J., 2009. Low osmium solubility in silicate at high pressures and temperatures. Earth Planet. Sci. Lett. 279 (3-4), 165–173.

Young, E.D., Kohl, I.E., Warren, P.H., Rubie, D.C., Jacobson, S.A., Morbidelli, A., 2016. Oxygen isotopic evidence for vigorous mixing during the Moon-forming giant impact. Science 351 (6272), 493–496.

Zindler, A., Hart, S.R., 1986. Chemical Geodynamics. Annu. Rev. Earth Planet. Sci. 14, 493–571.

Zindler, A., Jagoutz, E., Goldstein, S.L., 1982. Nd, Sr and Pb isotopic systematics in a three-component mantle: a new perspective. Nature 298 (5874), 519–523.